DERIVATION AND USE OF FORMULATIONS FOR FRAMING DESIGN IN THE POLAR CLASS UNIFIED REQUIREMENTS

Prepared for:

IACS Ad-hoc Group on Polar Class Ships
Transport Canada

Prepared by:

A. Kendrick, AMARK Inc.
C. Daley, Daley R&E

January, 2000

TABLE OF CONTENTS

TERMINOLOGY

Ω	smallest angle between the chord of the waterline and the line of the first level of framing
τ_c	critical buckling stress in shear
τ_a	applied vertical shear stress
σ_a	applied vertical bending stress
σ_c	critical buckling stress in compression, according to UR S11.5
σ_u	specified material ultimate tensile strength
σ_y	minimum material upper yield stress
a	main frame span
AF	Area Factor
A_f	area of flange
A_m	minimum main frame web area
$A_{m\ FIT}$	web area of main frame as fitted
A_t	total area of stiffener
b	(1) height of the rectangular ice load patch (2) width of outstand of flanged section
b_{eff}	width of shell plating that acts effectively with a framing member
b_t	breadth of bulb plate flange section
c_x	distance from the shell plating to the centre of gravity of the stiffener
E	modulus of elasticity
F	total glancing impact force
h_w	height of web
j	number of fixed support end conditions (equal to 0, 1 or 2)
KA	coefficient accounting for effect of frame cant
$k_{a1,2,3}$	coefficient account for location of the section equal area axis
L	ship length (Rule Length as defined ins UR S2.1)
LL	length of loaded portion of span
OF	frame orientation factor
P	Pressure
P_{avg}	average pressure
PC	Polar Class
PPF	peak pressure factor
Q	line load
s	main frame or longitudinal spacing
t	as built plate thickness
t_c	corrosion allowance for internal structures
t_f	thickness of flange
t_{min}	required minimum shell plate thickness
t_{net}	plate thickness required to resist ice loads
t_w	web thickness
t_{wear}	thickness addition for corrosion and/or ice-induced abrasion
UR	IACS Unified Requirement
w	width of the rectangular ice load patch
zp	sum of plastic section moduli of flange and shell plate as fitted
Zp	plastic section modulus of frame section including effective plating as fitted
Zpr	Reduced plastic section modulus in combined bending and shear
$Z_{pm\ FIT}$	plastic section modulus of main frame as fitted
$Z_{pm\ min}$	minimum required plastic section modulus of main frame

1. INTRODUCTION

This document describes how the IACS Polar Class Unified Requirements have been developed. It explains how the principles for design and analysis were established, how design cases were identified, and how systems of equations describing these were formulated and compared with predictions from finite element models. Examples illustrating results are presented, illustrating trends with polar class, frame spacing and span. Other examples also show how well balanced certain existing designs would be against the new criteria.

The full derivations of many of the UR equations are quite complex. They are presented in Annexes to the report. A number of documents are noted as references. Many of these were produced during the UR development process. They provide more details of the rationale behind the selection of the methods and assumptions presented here.

2. PLASTIC DESIGN AND DESIGN CRITERIA

2.1 Rationale for Plastic Design

Several current sets of ice design rules and standards, including those of the Russian Maritime Register (MRS, [1]) and those of the Canadian Administration (CASPPR, [2]) use plastic design methods. This is unusual in ship design, where most traditional rule formulations are based on elastic criteria. There are several elements to the rationale for the use of plastic design for ice-structure interaction. These include:

- Using plastic design can help ensure a better balance of material distribution to resist design and extreme loads. This is particularly important because extreme ice loads can be considerably in excess of design values. This is more likely for ice loads than (for example) for wave loadings. The use of plastic methods ensures a considerable strength reserve, which may or may not be the case with elastic design.
- Plastic design can allow considerably lighter structure, particularly when the return period for design loads is relatively long and when cumulative damage (deformation, fatigue cracking, etc) is not a major consideration.
- Plastic design methods are more applicable to damage analysis, which will allow the assumptions in the URs to be tested against experience and refined in future as necessary.

These considerations tie in well with the design scenarios and load models developed for the URs [3, 4], and with actual operating practice for ice class ships. Occasional local deformation (denting) has tended to be an acceptable consequence of ice operations, provided that this does not compromise the overall strength or watertight integrity of the ship.

2.2 Acceptable Limit States

The selection of structural design criteria for plastic design is more difficult than in elastic design. In the latter, first onset of yield is relatively easy to predict, and thus offers a simple criterion for design. In plastic design, there are many possible limit states ranging from yield through to final rupture.

There are various ways of describing the design limit states used in the UR proposals. Nominally, the limit states are plastic collapse mechanisms. However, they are quite simplified mechanisms. For several reasons the real structure will not collapse like the assumed mechanism. The main reasons are that the assumed mechanism ignores the beneficial effects of membrane stresses and strain hardening. As a consequence the real structure will have a substantial reserve beyond the design condition. More precisely then, the design limit state represents a condition of substantial plastic stress, prior to the development of large plastic strains and deformations.

The points at which the initial changes in stiffness can be expected can be predicted with reasonable accuracy by relatively straightforward analytical methods. The methods

selected to derive the URs are energy methods, which balance external and internal work under certain loading and response mechanisms, as described below. Unfortunately, such methods can not provide deflection or strain predictions, and so it has been necessary to rely on finite element methods to 'calibrate' these aspects of the design criteria and procedures. Specific examples of how this has been done are noted below.

The actual formulae are directly derivable from rigid-plastic energy-based collapse analysis methods. This type of analysis employs small-deflection assumptions and therefore excludes the strength reserve mechanisms (membrane, stain hardening) mentioned above.

Full non-linear finite element analysis has been used to verify the formulae and show the level of reserve strength. At the design limit states the structures lose stiffness, but are still able to carry higher loads. Figure 2.1 illustrates the behaviour of a typical frame, and Figure 2.2 provides an associated FE analysis.

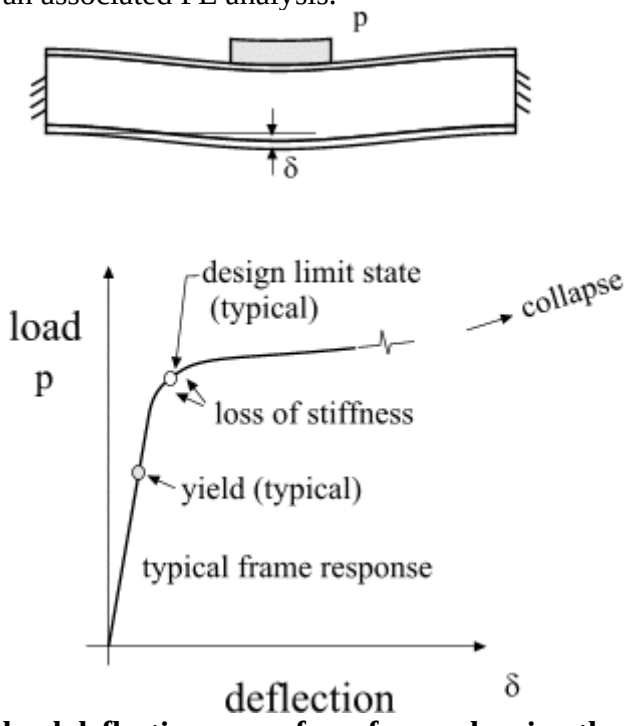

Figure 2.1 Typical load deflection curve for a frame showing the design point.

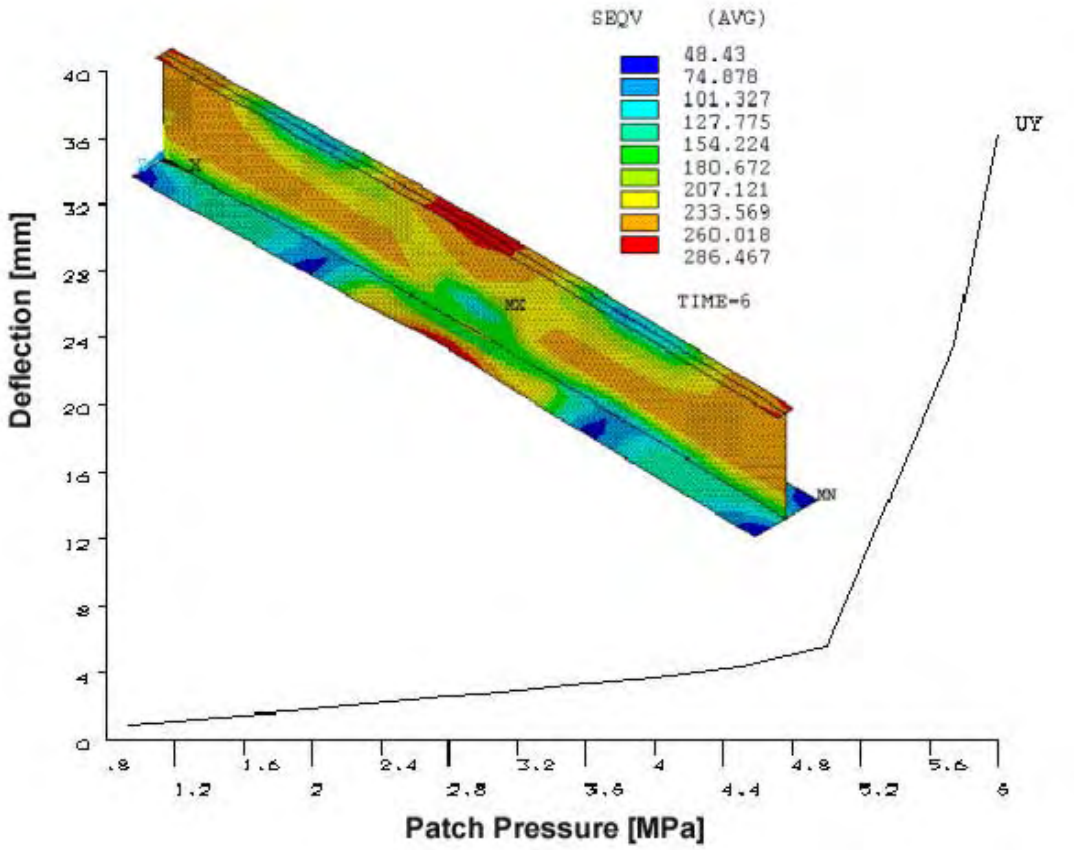

Figure 2.2 Load vs. Deflection and state of stress for a typical ice frame.

2.3 Energy Methods and Associated Issues

Energy methods provide a powerful analytical tool. However, some features of energy methods should be understood by their users.

In order to apply the method, a response mechanism has to be selected. There are many possible mechanisms for any load/structure combination, and it is necessary to find the one that gives the lowest structural capacity, as this will be closest to the capacity that the structure actually provides. Even if the lowest solution has been found, the represents the upper bound to capacity; i.e. the structure can do no better than this, and may well do worse. This statement is true as long as the postulated mechanism is valid for the boundary conditions and if the material is ideally plastic. In the absence of other factors, energy methods produce non-conservative results.

Counterbalancing these potential sources of non-conservatism, energy methods (as normally applied) do not include all components of any response. Typically, they assume elastic/perfectly plastic material response and thus exclude both membrane and strain hardening effects. These are small in the initial stages of response but provide

considerable reserves of strength when the structure deflects significantly – this shows up clearly in figures 2.1 and 2.2. Several other sources of load-bearing capacity may also be ignored for reasons of simplicity. In addition, approval procedures for the steels specified for polar ships will ensure that their specified material properties are lower bounds to their actual capacity. Thus, although the mechanisms describing response may appear to permit 'collapse', the actual collapse load will be significantly in excess of the 'mechanism formation' load.

The energy methods utilized in deriving the URs take account of the following possible energy-absorbing mechanisms:

1. a pure bending hinge;
2. a combined shear/bending hinge;
3. a shear hinge;

The interactions of bending and shear are described at section 3.2.

3. DESIGN CASES AND MECHANISMS

3.1 Assumptions

All of the structural design requirements are based on the UR load model, described in a companion document [3]. This model assumes a load patch of constant intensity in the vertical direction, peaked longitudinally. For use in plate, frame, and grillage design the load representation is in all cases simplified to a uniform rectangular patch.

The load is assumed to be applied to an ice-strengthened area of the hull, with a magnitude and distribution determined by polar class (1-7), hull area (bow, midbody, etc) and hull shape (in some hull areas only). Within the ice-strengthened areas it is assumed (and required) that stiffeners terminate in a manner that provides full fixity. Intersections with deep members, decks, bulkheads etc are designed to provide sufficient connectivity to offer the same restraint.

The basic design equations assume that frame members have uniform cross-sections along their length (see below for treatment of brackets). It is also assumed that all structure has the same material properties, e.g. yield strength is identical for plating and framing. When this is not the case, section properties need to be adjusted as appropriate.

A final assumption used in many of the calculations is that the position of the plastic neutral axis of a frame cannot move inside the attached plate, although the equal area axis (nominally the same thing) will frequently be within the plate. Stress/strain compatibility makes a locus within the plate impossible in practical terms, and the same assumption has been used in other rule systems, for example the CASPPR [2]. However, in the URs the neutral axis is permitted to be above the plate, which is not the case in CASPPR. This removes a potential source of non-conservatism for certain (unusual) structural configurations.

3.2 Bending and Shear Interaction

In most structures, elements support a combination of bending and shear loads and associated stresses. A frame carrying shear load will have less bending capacity than one in pure bending; likewise when bending stresses are present full shear capacity is no longer available. This interaction is recognized in the MRS ice class rules [1] but not under ASPPR [2]. In the latter case the two capacities are calculated and applied independently.

The current UR proposals treat bending and shear interaction more rigorously than any existing rules or standards, by taking into account actual section shape in the calculation procedure. This can be represented by equation 3.1 [5], where α is section-dependent, and greater than or equal to one.

$$\left(\frac{M}{M_{ult}}\right)^2 + \left(\frac{T}{\alpha \,.\, T_{ult}}\right)^2 = 1 \qquad \ldots(3.1)$$

Bending moment, M, and Shear, T have actual and ultimate values as indicated. Reviewing this equation, and the curve that can be used to represent it (figure 3.1) it can be seen that at full shear any section with $\alpha > 1$ will have some reserve bending capacity.

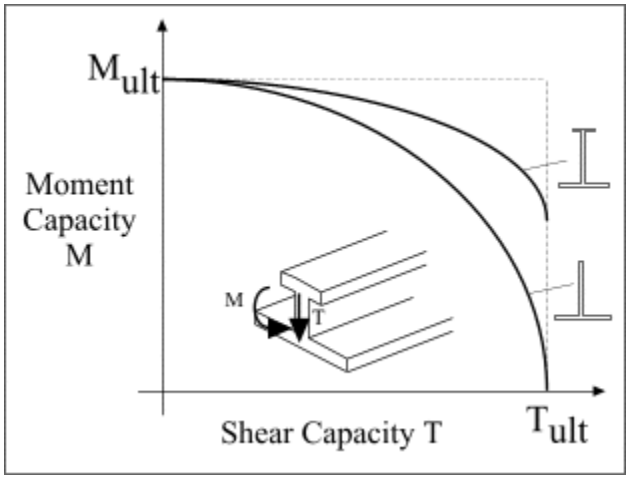

Figure 3.1: Bending/shear interaction diagram

How this is established in the URs is described in full in Annex A. To summarize, it is assumed that any section has a web and one or two flanges. The attached plate constitutes the 'fixed' flange, and the other (if any) the 'free' flange.

Only the vertical part the stiffener is assumed to contribute to shear capacity, but for a variety of reasons the full height is taken as contributing to the shear area, not merely the web as normally defined. In the description that follows, 'web' is taken as referring to this full height or depth. As the shear capacity of the web is used up, the moment capacity of the section reduces until, at the full shear condition , the residual section modulus is defined by the free flange contribution only. Thus, a flat bar has no residual capacity, whereas a stiffener with flange area equal to web area would retain 2/3 of its initial moment capacity. This approach is only applicable up to the point where the web yields fully and forms a shear hinge. Beyond that point, a different approach is needed, as described below.

In a pure bending hinge, the interaction between shear and bending is not an issue, and in a combined hinge it is dealt with as described. The shear hinge has required some additional consideration in order to allow reasonably full treatment of some response mechanisms beyond the full shear condition described above. When a shear hinge is assumed to form by fully yielding the web, the flanges can still provide additional load bearing capacity. In a truly pure shear collapse, the total areas of these flanges would also need to reach yield. However, there will normally be a lower energy collapse path involving localized bending hinges in each of the flanges. These local hinges form part of the assumed response mechanisms for the asymmetrical case described below. In the

symmetrical case (centred load) shear hinges are ‘designed out’, and the local hinges can be omitted.

To be more accurate, all the combined bending/shear hinge models could include a progressive flange hinge allowance of this type. As the web yields, the modulus calculation takes less of the attached flange (plate) contribution into account, and so this could be added back into the equations. For any polar class ship the magnitude of the contribution will amount to a few percent, and it is considered more appropriate to limit the complexity of the design equations and leave this as a strength margin. It can be noted that in the latest MRS rules, a potentially substantial flange effect is included. However, under that approach, only a reduced ‘α’ factor is allowed, and the overall effect is thus similar for section shapes typical of Russian practice.

3.3 Load Cases

During the development of the URs, there was considerable debate regarding the selection of design load cases. However, there was never any dispute that one of these should be the centred load case, where the ice load is applied at mid-span of the frame, as shown in figure 3.2.

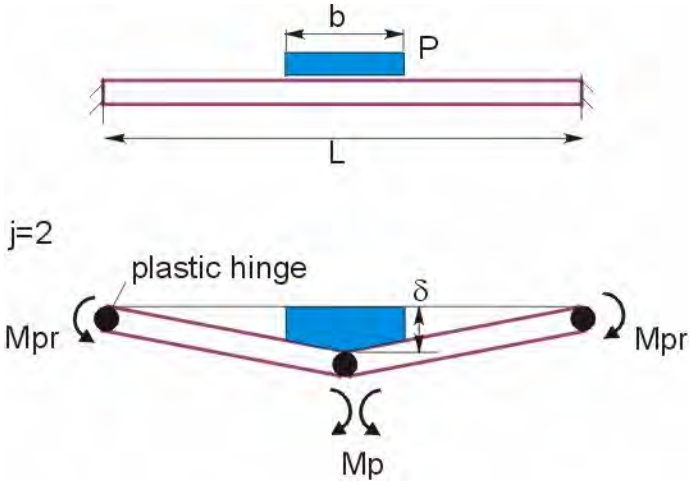

Figure 3.2: Symmetrical (centred) load

The second case forming part of the UR system has the load concentrated towards one end of the frame, as in figure 3.3. Work during the development process demonstrated that this may giver lower collapse loads for certain cases. The dominant mechanism will depend on the section shape and on the load length and intensity.

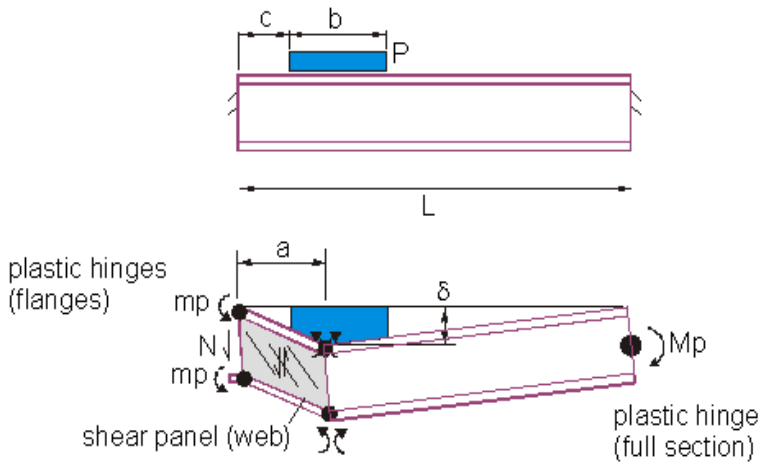

Figure 3.3: Asymmetrical (end) load

4. SYMMETRIC LOAD CASE

4.1 Selection of 3-Hinge Mechanism

There are several possible response mechanisms under the centred load, including:

- 3-hinge bending/shear;
- 4-hinge bending/shear;
- 2 shear hinge;

These are illustrated in figure 4.1

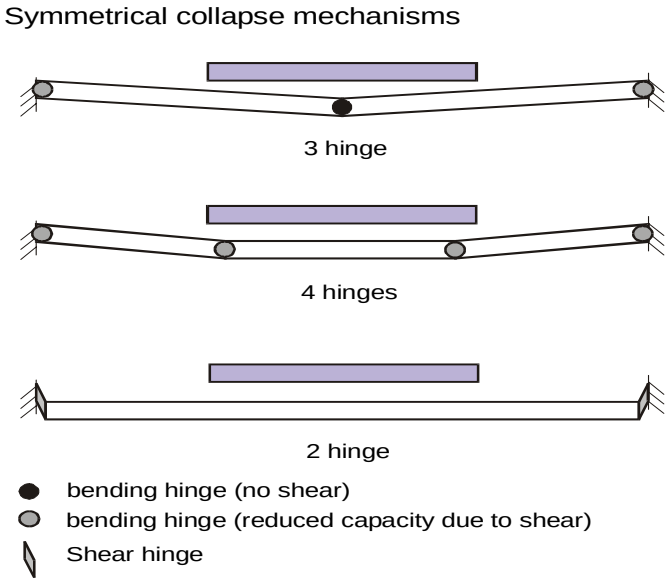

Figure 4.1: Symmetrical Collapse Mechanisms

Solutions for the 3 and 4 bending/shear hinge response were developed and compared, and it was concluded that the 3 hinge normally dominates, or else is sufficiently close to the 4 hinge to be used as a proxy for this. In principle, higher numbers of hinges may give lower capacities still, but the differences from the 3-hinge solution always seem to be acceptably small. This conclusion has been validated by a large number of finite element analyses of centred load cases, in all of which the 3-hinge allowable load falls slightly below the loss-of-stiffness knuckle.

The 3-hinge mechanism involves two bending/shear hinges at the ends (except when one end is simply supported – see below), and one pure bending hinge in the middle. These are combined as described in 4.4.

4.2 Special Case – Shear Collapse

In principle, a centred load could result in the formation of either a 2 or 4 shear hinge mechanism, with or without flange hinges (see asymmetrical case). However, the proposals preclude this by setting the minimum permissible web area at a value just

corresponding to full shear. This ensures that the design point can be defined by the 3-hinge mechanism described above. (though at minimum shear area the 2- and 3-hinge solutions are identical).

This does not imply that shear collapse under higher loads is impossible, and it may indeed take place. There is sufficient conservatism built into the shear response mechanisms for the centred load case to mean that a considerable reserve of strength exists in this scenario.

4.3 Special Case – Simple Support

As noted, it is possible that an ice frame will have only one end fixed and the other (outside the ice belt) simply supported. Under these conditions the hinge system has a single bending/shear hinge at the fixed end and the same pure bending hinge at the centre. This has been provided for by introducing a frame support coefficient, j, to the rule equations (j = 1 or 2 fixed ends).

In principle, a more sophisticated treatment of this situation would show that the worst location for the load would be closer to the simple support, and a different and more complex set of equations would be needed to define the system. In practice it is highly improbable that such a loading would apply, as the icebelt already extends above the waterline and peak loads are unlikely to be seen in this area, especially higher up. Therefore, the additional complexity of a tailored solution is considered unnecessary.

4.4 Derivation of Requirements

The full derivation of the UR formulae is provided at Annex A. In summary, following the approach outlined above, the steps include:

.1 define the minimum web area required to carry the load in pure shear.

$$Ao = \frac{1}{2} P \cdot b \cdot S \cdot \frac{\sqrt{3}}{\sigma_y} \qquad \ldots(4.1)$$

.2 develop the energy balance equation for external and internal work

$$(P \cdot b \cdot S)\left(1 - \frac{b}{2 \cdot L}\right) = 4 \cdot \frac{\sigma_y}{L} \cdot \left(Zp + \frac{j}{2} \cdot Zpr\right) \qquad \ldots(4.2)$$

.3 establish the full plastic section modulus, Zp for the centre hinge

$$Zp = Af \cdot \left(\frac{tf}{2} + hw + \frac{tp}{2}\right) + Aw \cdot \left(\frac{hw}{2} + \frac{tp}{2}\right) \qquad \ldots(4.3)$$

(note that the full version of these equations takes account of several options for the locus of the neutral axis.)

.4 establish the reduced section modulus, Zpr for the end hinges, including the section shape dependency effect;

$$Zpr = Zp \cdot \left[1 - kw \cdot \left[1 - \sqrt{1 - \left(\frac{Ao}{Aw} \right)^2} \right] \right] \qquad \ldots(4.4)$$

where $kw = \dfrac{1}{1 + 2 \cdot \dfrac{Af}{Aw}}$

.5 combine the capacities to provide a section load limit formula

$$P = \frac{\left[j + 2 - kw \cdot j + kw \cdot j \cdot \sqrt{1 + 3 \cdot (j + 2) \cdot Zpns \cdot (-j + 2 \cdot kw \cdot j - 2)} \right]}{6 \cdot Zpns \cdot kw^2 \cdot j^2 + 2} \cdot \sigma_y \cdot Zp \cdot \frac{4}{\left[b \cdot S \cdot L \cdot \left(1 - \dfrac{b}{2 \cdot L} \right) \right]} \qquad \ldots(4.5)$$

where $Zpns = \left[\dfrac{Zp}{Aw \cdot L \cdot \left(1 - \dfrac{b}{2 \cdot L} \right)} \right]^2$

Equation 4.5 is not yet in a rule form. It can be used directly in comparisons with those of finite element models or experiments; as for example in figure 4.2., Full model details are given at Annex A. As can be seen, the equation slightly underpredicts the loss of stiffness load, and thus relates to plastic strains of fractions of a percent and to very small residual deflections. These are all desired characteristics for the design point, and thus this capacity equation is considered to offer a valid basis for the required UR formulations.

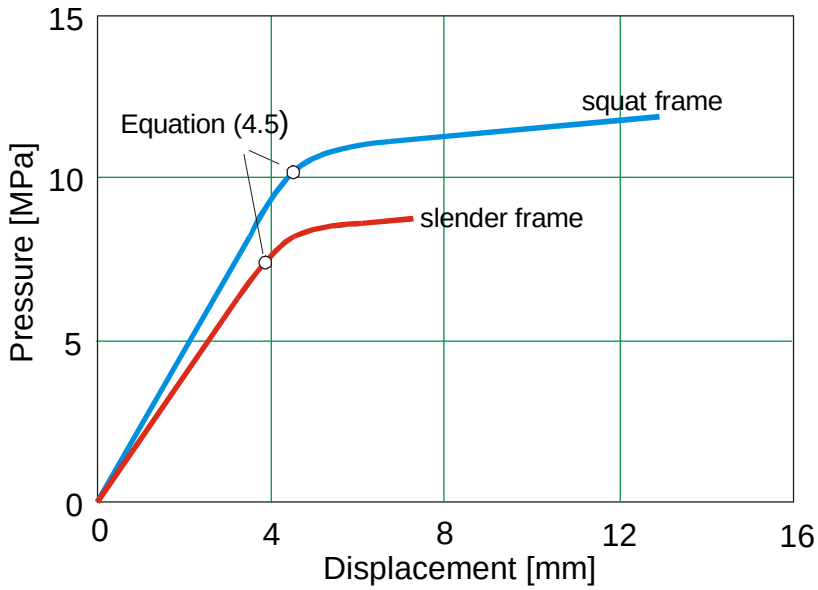

Figure 4.2: Analytical and FE responses

An examination of the form of the capacity equation shows that it contains multiple unknowns, and thus the UR version provided at Section 7 does not offer a closed form solution. For any general configuration (frame span and spacing) it is necessary to iterate to an acceptable section shape to resist the design load. Structural optimization therefore becomes somewhat more complicated than is the case in the majority of current ice class rule systems. However, the procedures are more rigorous and consistent than those of any current system.

The influence of brackets has been investigated by additional finite element analyses, and it appears that it is generally acceptable to take effective frame span as being between bracket toes. Classification society practices differ somewhat, but any of their approaches will give a conservative result on this basis.

5. ASYMMETRIC LOAD CASE

5.1 Selection of Mechanism

As noted at 3.3, the asymmetric (end) load case will not normally govern frame capacity requirements, but may do so for certain structural configurations. The way in which the requirements for this load case have been developed essentially allows the centred load case to provide many of the constraints for the design domain, and checks that the asymmetric requirements are also fulfilled.

A full collapse initiation mechanism for this case, analogous to the 3-hinge case for the centred load, is shown at figure 5.1. However, the way in which this mechanism develops differs considerably from the centred load case. There, the formation of the hinges is virtually simultaneous, leading to a rapid loss of stiffness, as shown in the plots at figure 4.2. In the asymmetrical case, the order of hinge formation normally develops the shear hinge at the closer support at a significantly lower load level than that for the bending hinge in the span. As a result, the local plastic strains (and residual deformations after unloading) can be much larger than those in the centred load case (though still normally quite small in absolute terms).

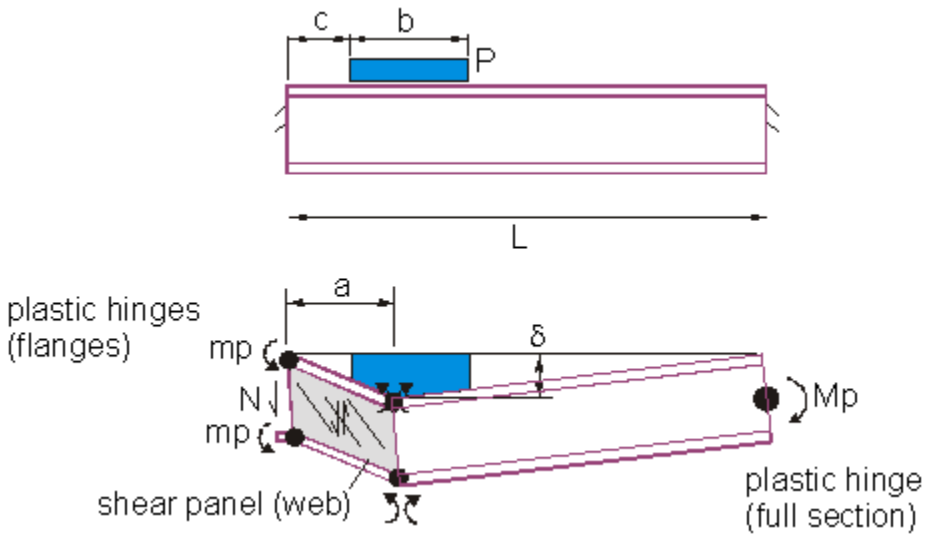

Figure 5.1: Asymmetrical Collapse Mechanism

This is illustrated in figures 5.2 (drawn from ref [6]), which shows the response of a frame to both a centred and an end load, as calculated by F.E. methods and compared to 'collapse initiation' analytical solution. The end load analytical equation used in this case is a less conservative solution than that proposed in the URs, and as a result it can be seen that a significant loss of stiffness in the asymmetrical case occurs considerably before the predicted collapse (ultimate) load. Associated with this, the residual deformation after unloading would be much higher with this analytical design point for asymmetrical loads

than is the case for the symmetrical loads.

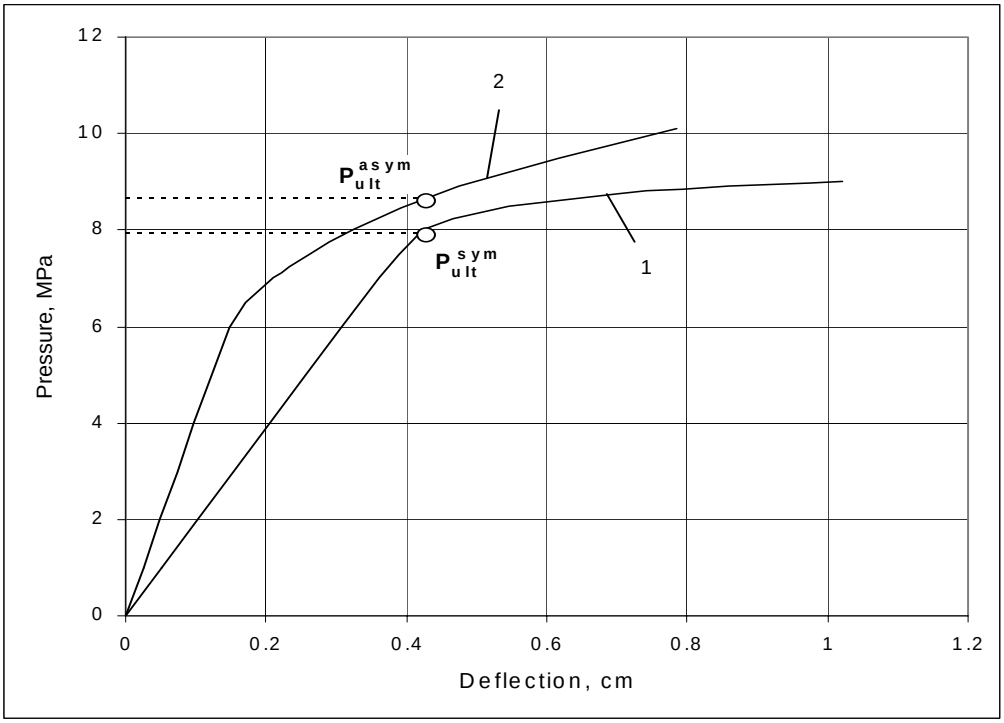

Figure 5.2: Comparison of responses under analytical 'collapse' loads

Other F.E. studies show that the initial knee in the asymmetrical response curve corresponds to an end shear hinge. The end shear condition could be used to define asymmetrical load requirements, but this provides a more conservative approach than that accepted for the centred load. Several other features of figure 5.2 and its companion 5.3 should also be noted. First, figure 5.2 shows that the 'residual stiffness' under asymmetric load is generally significantly higher than that for the symmetric load, and the ultimate load capacity is likely to be higher. This is borne out by figure 5.3, which shows local plastic strains at the ends and under the load. As with the overall deflection, local strain starts to build earlier for the asymmetrical case, but does so more slowly. Global or local collapse will both require higher loads under the asymmetrical load for this frame, and for any others that have been analyzed extensively in the background work for the URs.

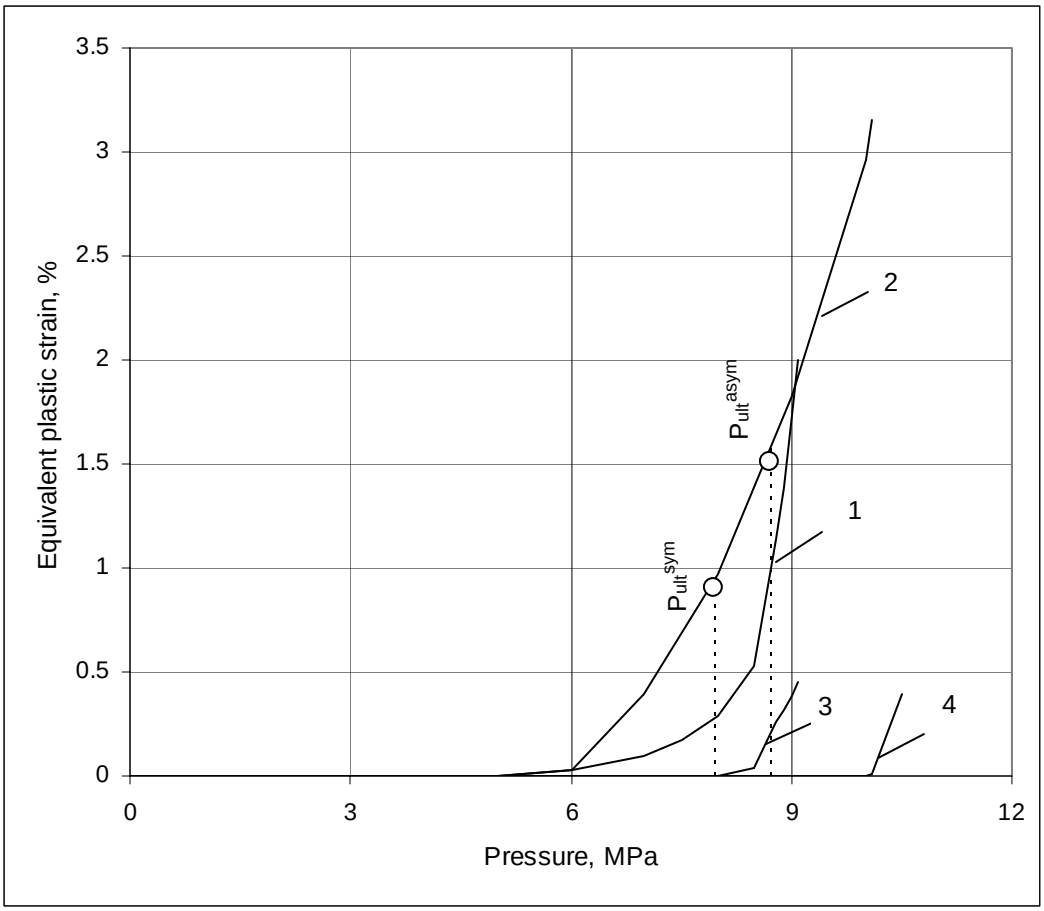

1 – local strain in the supporting section area under symmetric load
2 – in the supporting section area under asymmetric load
3– in the span middle under symmetric load
4 – in the section M = M_{max} under asymmetric load

$\mathbf{P_{ult}^{sym}}$ - design load from fig 5.2 under symmetric load

$\mathbf{P_{ult}^{asym}}$ - design load under asymmetric load

Figure 5.3: Development of local strain

Consideration was therefore given to defining a stage in the development of the collapse mechanism falling between the shear hinge and full collapse initiation. The approach selected is as shown in figure 5.1. It assumes that the shear panel formed between two shear hinges has started to deflect to a point where the flanges of the section are acting as independent bending hinges (as outlined at 3.2) but before this generates sufficient deformation to require the full bending hinge further along the section. Interestingly, as shown in Figure 5.1 the minimum energy solution for this mechanism does not normally have the load right at the support, but starting some distance along the frame, in order to allow the flange hinges to develop.

Since substantial deformations are impossible with this mechanism, it was assumed that it would keep strains and deflections within acceptable limits. Figures 5.4 illustrates the actual outcome. 5.4 is based on the same frames as Figure 4.2, and shows how the new

limit load relates to the load deflection curve. A comparison of the two figures will show that for this assumed load configuration, both frames are dominated by the asymmetrical loading case, but this is not always the case.

In many configurations, substantial components of an end load will be transmitted directly into the supporting structure perpendicular to the frame, rather than by the frame itself, as assumed here. Several existing classification society rule systems have procedures for reducing the load under these circumstances. The UR approach does not take account of this for several reasons, including the poor fit of 'standard solutions' to the response mechanism, and to the more complex treatment of brackets that might become necessary.

5.2 Derivation of Requirements

The full derivation of the UR formulae is provided in Annex B. The steps can be summarized as:

.1 balance the external and internal work:

$$(P \cdot b \cdot S)\left(1 - \frac{b}{2 \cdot L}\right) = \sigma_y \cdot \left[\frac{Aw}{\sqrt{3}} + \frac{Zp}{L} \cdot fz\right] \quad \ldots(5.1)$$

where *fz* can be approximated as:

$$fz = 1.1 + 5.75 \cdot kz^{.7} \quad \ldots(5.2)$$

and *kz* is the ratio of the combined flange moduli to the total section modulus:

$$kz = \frac{zp}{Zp} \quad \ldots(5.3)$$

.2 reformulate to develop the capacity equation for the frame:

$$P = \frac{\sigma_y}{b \cdot S\left(1 - \frac{b}{2 \cdot L}\right)} \cdot \left[\frac{Aw}{\sqrt{3}} + \frac{Zp}{L} \cdot (1.1 + 5.75 \cdot kz^{.7})\right] \quad \ldots(5.4)$$

Equations 5.4 and 4.5 govern the asymmetrical and symmetrical load capacities respectively, and are combined in the rule equations are shown in Section 7. Figure 5.4 shows the capacities predicted by equations 5.4 for the same two frames used to illustrate the symmetrical response.

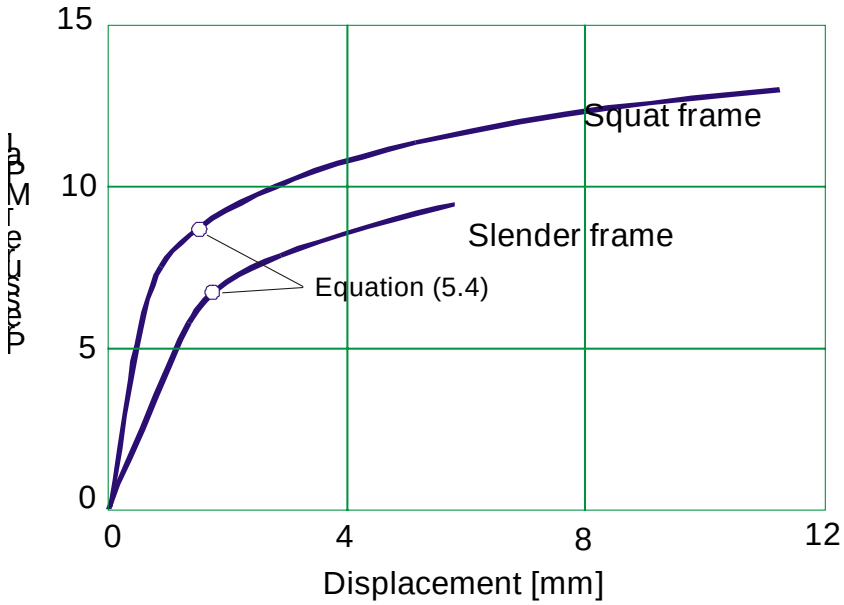

Figure 5.4: Asymmetrical Response

6. STRUCTURAL INSTABILITY

6.1 Introduction

In order for sections to achieve the plastic limit states defined above, it is necessary that they do not fail prematurely due to instability mechanisms such as buckling or tripping. Failures of this nature have frequently been observed in ice-going ships. They are particularly undesirable in that they can lead to extensive collapse with little or no increase in load level, unlike the mechanisms described earlier which have material and geometric strength reserves.

A considerable amount of research into instability under (simulated) ice loads has been undertaken, using both experimental and numerical methods (refs [7], [8]). This work has indicated that it is generally sufficient to prevent instability in the elastic response regime, for reasons that remain imperfectly understood for at least some of the mechanisms involved. However, the outcome is that the instability requirements in the URs can be drawn from existing IACS/class rules in most cases. Their form is thus reasonably familiar.

An examination of the stability criteria below shows that they constrain the design space for most frame designs significantly. If a designer is working with standard sections (bulbs, or Ts other than fabricated shapes) these will add further constraints; and it should be verified that any series will meet the stability criteria given the wastage allowances that also apply (see ref. [9]).

6.2 Treatment of Angled Sections

The responses described at Sections 4 and 5 assume that sections are symmetrical (or nearly so) about the axis of application of the load; i.e. they are Ts, flat bars, or bulbs normal to the shell plating. When any of the above sections is not normal, it will lose effectiveness in bending and shear; and correction factors for this are included in the URs. It will also tend to 'trip'; i.e. to rotate further from the normal towards the plate. This is prevented in the URs by requiring the fitting of tripping brackets at close spacing, whenever the angle from the normal exceeds 15 degrees (see section 7).

Angle sections will always display these asymmetrical behaviours, and their use in polar class ships is not recommended. Wherever they are used, brackets are again required.

6.3 Web Instability

Web instability occurs when shear stresses exceed buckling limits. The behaviour is considered to be reasonably well predicted by relatively standard flat plate formulae. These show much better performance for sections with attached flanges (i.e. T-sections, angles, and bulbs) than for flat bars. The general buckling formula are:

For flat bar sections: $h_w / t_w \leq 282 / (\sigma_y)^{0.5}$

For offset bulb flat sections: $h_w / t_w \leq 805 / (\sigma_y)^{0.5}$
For tee sections: $h_w / t_w \leq 805 / (\sigma_y)^{0.5}$
For angle sections: $h_w / t_w \leq 805 / (\sigma_y)^{0.5}$

where: h_w = web height
t_w = net web thickness
σ_y = minimum upper yield stress of the frame material [MPa]

An effective flange; i.e. one that offers the necessary restraint, is provided automatically if the flange width criteria are observed. The minimum acceptable flange width is set at:

$$w_f \geq 5 \times t_w$$

Standard bulbs are also assumed to have acceptable properties in this regard. There is some experimental evidence to suggest that the flat bars are unduly penalized by these formulae, but insufficient data is available at this time to justify any relaxation.

For local failures near the web/plate intersection, an additional criterion is imposed for all sections, such that:

$$t_w \geq 0.35 * t_{ice} * (\sigma_y/235)^{0.5},$$

where σ_y = minimum upper yield stress of the shell plate material (MPa)

In practice, the web thicknesses will tend to be greater than these minimum values in order to respect the general web instability requirements and provide adequate shear area.

6.4 Flange Instability

Flange instability occurs when compressive bending stresses in the flange exceed buckling limits. To prevent this, limits are placed on the outstand of the flange from the web.

$$b / t_f \leq 100 / (\sigma_y)^{0.5},$$

where b = width of outstand
t_f = thickness of flange
σ_y = minimum upper yield stress of the frame material [MPa]

7. UNIFIED REQUIREMENTS

7.1 Summary of Formulae

The framing design criteria in the URs represent an inversion and a combination of the formulae presented at Sections 4 and 5 (and their respective Annexes), plus the instability criteria derived at Section 6.

Minimum shear area is defined by UR equation 9.1 as:

$$\mathbf{A_m = 100^2 * 0.5 * LL * s * (AF * PPF_m * P_{avg}) / (0.577\sigma_y)} \ (cm^2)$$

where A_m = minimum main frame web area [cm^2]
LL = length of loaded portion of span
= lesser of a and b [m]
a = main frame span [m]
b = height of design ice load patch [m]
s = main frame spacing [m]
AF = Area Factor from UR Table 5.3
PPF_m = peak pressure factor from UR Table 5.2
P_{avg} = average pressure in load patch from UR Equation 5.12 [MPa]
σ_y = minimum upper yield stress of the frame material [MPa]

Section modulus is then found from UR equation 9.2 as

$$\mathbf{(Z_{pm})_{min} = 100^3 * LL * Y * s * (AF * PPF_m * P_{avg}) * a * A_1 * KA / (4*\sigma_y)} \ [cm^3]$$

where, Z_{pm} = plastic section modulus of the main frame [cm^3]
$Y = 1 - 0.5 * (LL/a)$
$KA = 1 / \cos\theta$
θ = angle between the plane of the web and a perpendicular to the shell plating at the midspan of the section, if $\theta \leq 15$ degrees, KA to be taken as 1.0
A_1 = maximum of
$A_{1A} = 1 / (1 + j/2 + kw*j/2*[(1-a_1^2)^{0.5} - 1])$
$A_{1B} = (1 - 1/(2*a_1*Y)) / (0.275 + 1.44kz^{0.7})$
j = number of fixed support end conditions of the main frame
$a_1 = A_m / A_{m\,FIT}$
A_m = minimum main frame web area [cm^2]
$A_{m\,FIT}$ = web area of main frame as fitted [cm^2]
$kw = 1 / (1 + 2*A_f/A_{mFit})$
A_f = flange area of main frame web as fitted [cm^2]
kz = zp / Zp
zp = sum of individual plastic section modulii of flange and shell plate as fitted [cm^3]
$= w_f*t_f^2/4 + b_{eff}*t_{net}^2/4$

w_f = width of flange
Zp = plastic section of main frame as fitted [cm^3]

Section modulus for different section shapes is calculated according to UR equations 8.1 – 8.3.

The instability criteria are covered in UR equations 14.1, etc and are identical to those listed in Section 6.

7.2 Application

The form of the equations above is such that they cannot be used directly to create a unique set of scantlings for a given overall configuration consisting of frame span and spacing, load patch dimensions and pressure. Finding any 'exact' solution will require iteration, and developing an optimum (for weight, or cost) will involve more complex calculations. However, checking the compliance of a new or existing design is quite straightforward. Where the scantlings are known, the 'achieved' shear area and modulus can be calculated directly and compared with the required values from the equations above.

A set of spreadsheets have been developed to facilitate the development of scantlings and comparisons with existing ships. A version can be downloaded from the site:

8. EXAMPLES

Three sets of examples are presented below and in the Annexes. These are;

1. A set of trend curves, showing section properties that just comply with the proposed URs;
2. A set of comparisons of rule solutions and FE analysis results, illustrating the nature of the design limit states;
3. A set of comparisons with existing ice-classed ships, showing how their frames compare with the new UR requirements.

In (1), the explorations have been made as systemmatic as possible, but this means that the section shapes are not always completely realistic or practical, though they do all comply with both strength and stability criteria. This also applies to some of the frames analyzed in (2). In (3), the existing ships are not necessarily built to rule minimum values, and are evaluated against a polar class that allows a full set of results to be developed for the scantlings. In the event that a reader wishes to undertake additional analysis to explore specific configurations or trends, a spreadsheet used in generating all these results can be obtained at the website

ftp://ftp.engr.mun.ca/pub/cdaley/Polar_Rules/.

8.1 Parametric Variants

A set of plots of shear area and section modulus requirements have been developed for some notional structural configurations, in order to illustrate key trends. The base case for all these calculations is a vessel of 30,000 tonnes displacement, with a traditional, relatively efficient icebreaking bow form. Loads have been generated for the bow and midbody areas for a range from PC 7 to PC 1.

A basic configuration of:

frame spacing	=	0.35 m
frame span	=	2.5m
steel yield strength	=	355 MPa
frame section	=	T
shear area ratio (bow)	=	1.1; i.e frames have 110% minimum shear area
shear area ratio (mid)	=	1.2

is assumed for the initial calculations of frame properties against polar class, shown in Figures 8.1(a) for the bow, and 8.1 (b) for the midbody. All results quoted are for net scantlings, and it should be recognized that all thicknesses used will need to be increased by 2 mm (or more) to meet the wastage requirements.

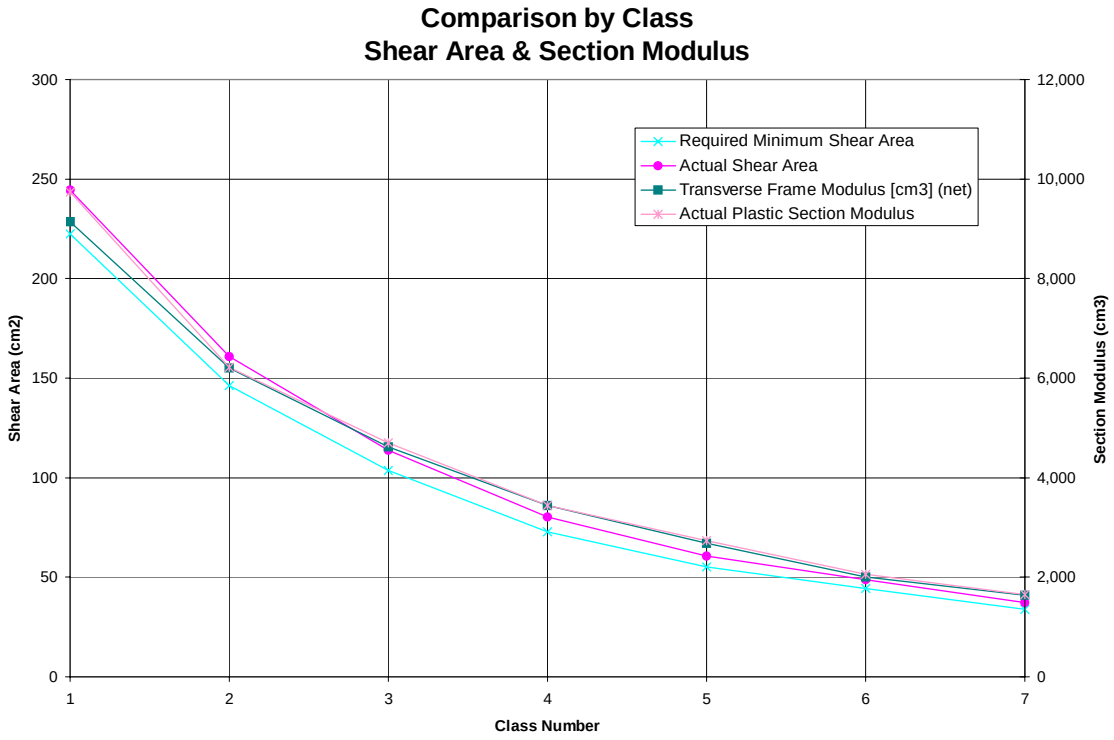

Figure 8.1a: Bow Frame Requirements

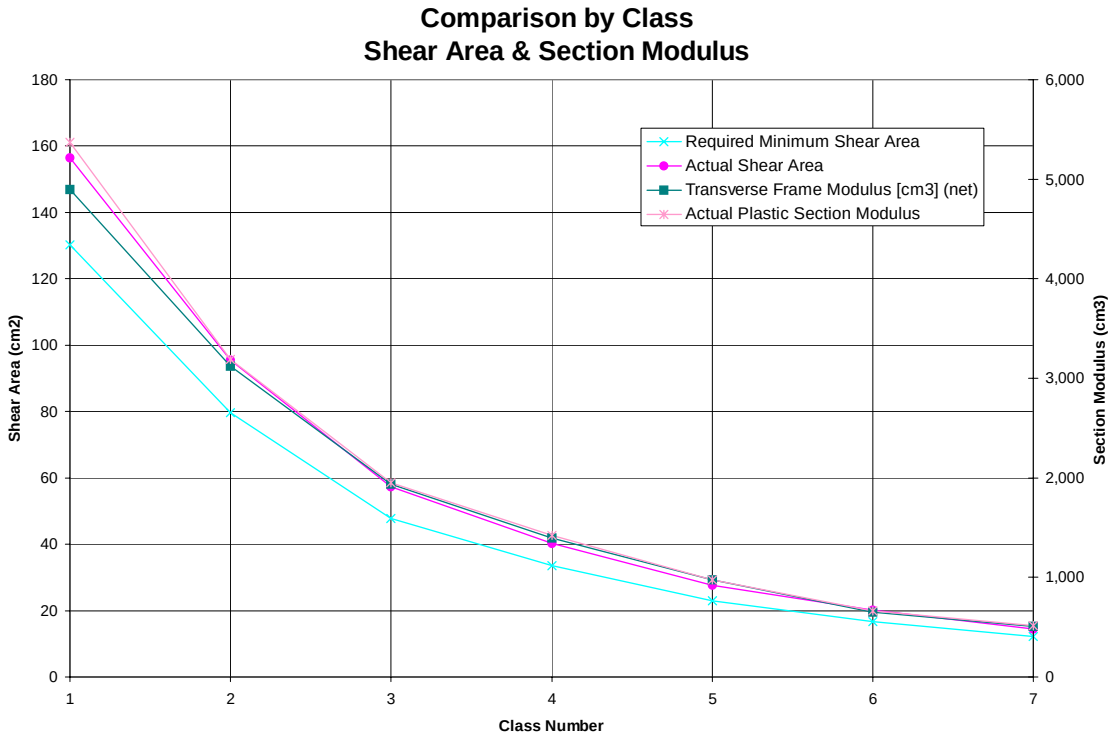

Figure 8.1b: Midbody Frame Requirements

In order to simplify the comparisons, all frames have been developed as follows. The web thickness is initially set at plate thickness, and flange thickness is the same. The required shear area is developed by giving the web adequate depth. The section modulus is then checked. If it is inadequate, the web depth is increased (and thickness reduced) and flange thickness and outstand are increased. The process is concluded when a section modulus between 1 and about 1.05 times the required value is generated, and when all other constraints (stability, etc) are respected.

The results are largely self-explanatory. The actual shear area is above the minimum possible value (by 10 or 20%) while the section modulus is a little above the target.

Additional calculations have been undertaken to illustrate how changing certain assumptions will change these results. All of these are based on the same vessel geometry, now at PC 4 class and 20,000 tonne displacement. Frame span is varied from 1.75 to 3.25 m, spacing from 300 to 600 mm, with most dimensional ratios kept constant. The results are shown in figure 8.2a and b, and in Table 8.1

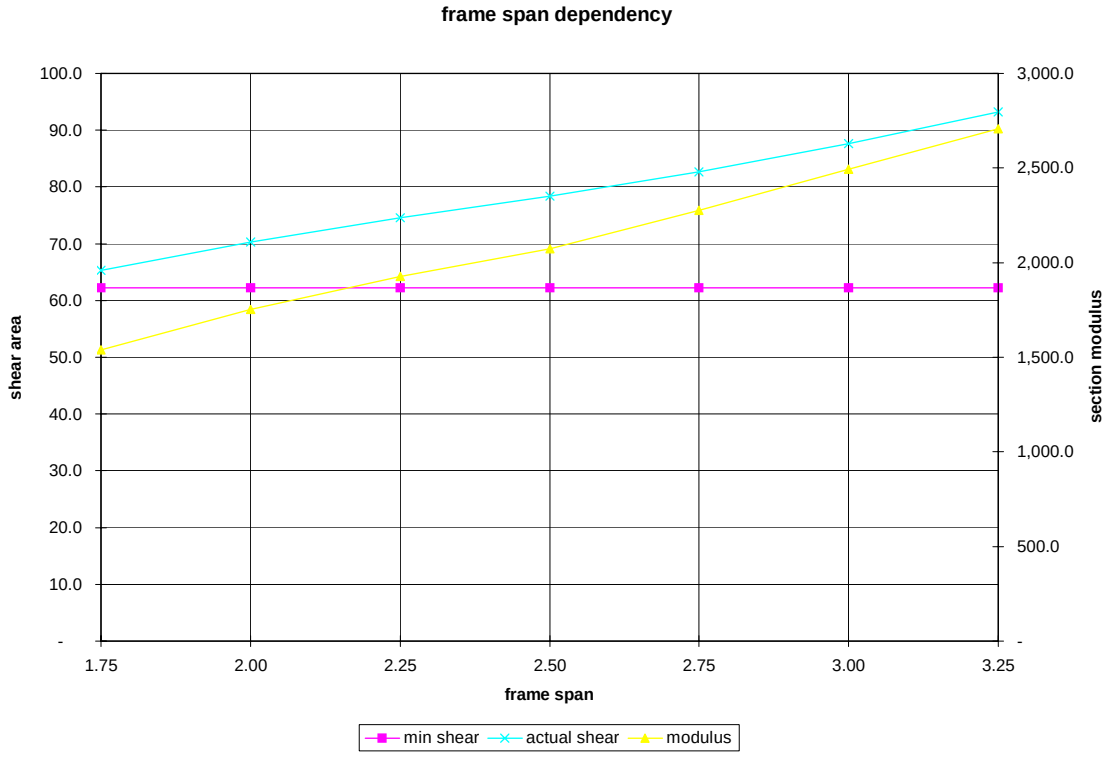

Note: varies only shear area ratio – all other ratios constant

Figure 8.2a: Frame Span Dependency

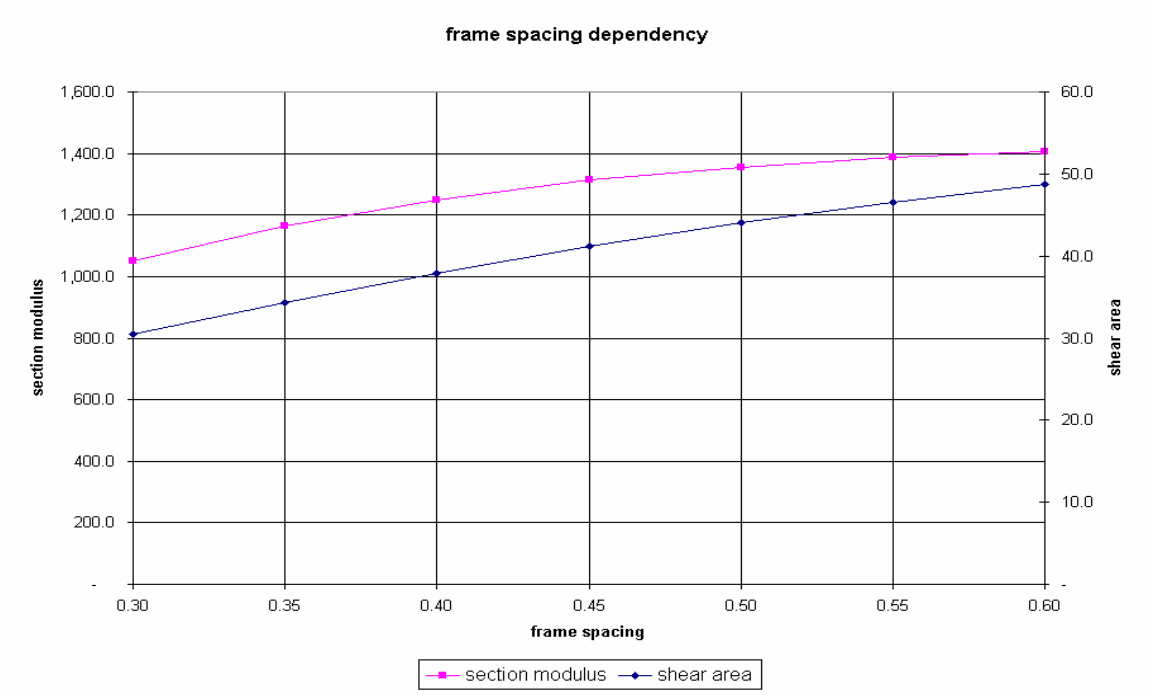

Note: varies only flange thickness and width ratios – all other ratios constant

Figure 8.2b: Frame Spacing dependency

Table 8.1: Frame Details

Frame spacing dependency						
fr_sp (m)	0.3	0.35	0.4	0.45	0.5	0.55
span (m)	2.5	2.5	2.5	2.5	2.5	2.5
tp (mm)	13.9	15.5	17.0	18.3	19.5	20.5
tw (mm)	13.9	15.5	17.0	18.3	19.5	20.5
hw (mm)	199.0	199.2	199.5	200.0	200.4	200.9
tf (mm)	20.8	22.5	23.8	24.7	25.3	25.7
wf (mm)	214.9	186.0	169.8	173.9	165.7	164.4
Frame span dependency						
fr_sp (m)	0.35	0.35	0.35	0.35	0.35	0.35
span (m)	1.75	2	2.25	2.5	2.75	3
tp (mm)	21.6	21.6	21.6	21.6	21.6	21.6
tw (mm)	21.6	21.6	21.6	21.6	21.6	21.6
hw (mm)	280.4	303.4	323.6	340.8	361.0	384.0
tf (mm)	21.6	21.6	21.6	21.6	21.6	21.6
wf (mm)	108.1	108.1	108.1	108.1	108.1	108.1

8.2 FEA Comparisons

Several dozen FE analyses have been undertaken to validate the analytical approach. Some examples were given above, using configurations previously presented and analyzed by other members of the IACS group. The similarity of the new results to the old was checked, to ensure that the modelling approach was valid and acceptable.

Additional FEA results are provided below and at Annex C. The set shown here in Table 8.2 and the example in Figures 8.3 are in the bow of the 30,000 tonne ship, for each of the seven classes. The ps and p3h entries give the analytical values for the asymmetrical and symmetrical load cases respectively.

Table8.1. Parameters of frames

30kT, Bow

var \class	C1 (PC1)	C2 (PC2)	C3 (PC3)	C4 (PC4)	C4a (PC4)	C5 (PC5)	C6 (PC6)	C7 (PC7)
b [mm]	1220	1180	1120	1060	960	1010	1110	1000
hw [mm]	620.8	547.3	511.8	484.1	409.9	444.3	411.6	345.3
tw [mm]	37.5	37.8	21.1	15.8	21.6	13	11.3	10.2
wf [mm]	187.3	138.8	147.8	142.3	108.1	142.8	124.1	143.2
tf [mm]	31.8	31.9	27.5	22.9	21.6	22.1	20.3	19.9
tp [mm]	37.5	30.8	26.4	22.6	21.6	20.0	17.4	15.7
S [mm]	350	350	350	350	350	350	350	350
lf [mm]	2500	2500	2500	2500	3250	2500	2500	2500
fy [MPa]	355	355	355	355	355	355	355	355
ty [MPa]	205	205	205	205	205	205	205	205
ps [MPa]	**20.94**	**18.00**	**10.48**	**7.79**	**7.88**	**6.21**	**4.56**	**3.83**
p3h [MPa]	**22.32**	**19.47**	**10.55**	**7.98**	**7.61**	**6.44**	**4.72**	**4.04**

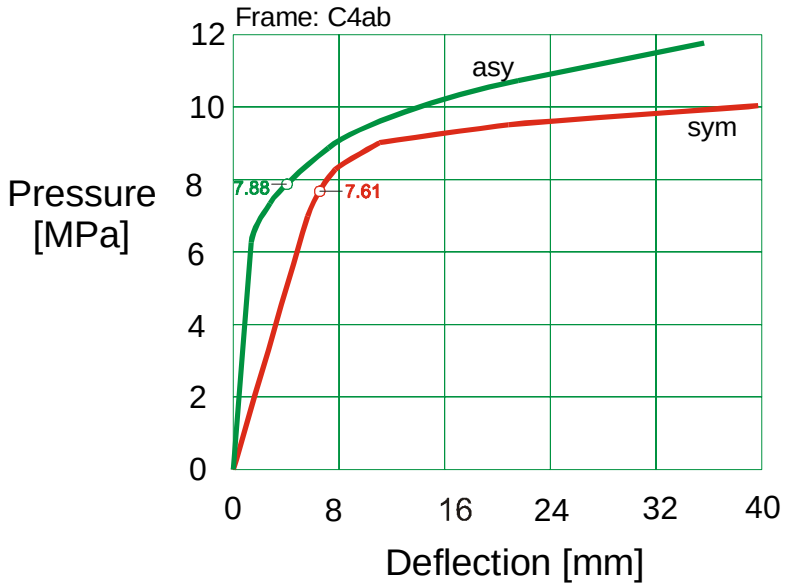

Figure 8.3a Load-deflection curves for frame C4a

Depending on the frame, the asymmetrical load/deflection curve may always be above the symmetrical curve, or the two may cross to give a region where a given load will give larger deflections for the asymmetrical case (see Annex C). When the latter situation holds, the analytical value for asymmetrical load capacity is always below the symmetrical solution, and in all cases checked to date it is at a level below the cross-over point.

8.3 Analyses of Existing Ships

Table 8.3 presents a selection of existing ship scantlings that have been checked against the framing proposals. Half of these vessels were built to Baltic class, and the others to one of the existing polar rule systems. In the latter case, the polar class against which they are analyzed (shown) is nominal, and has been based on a rough match of plate strength.

These results are drawn from a broader analysis to show typical outcomes. In many cases, the names of the vessels are not indicated for reasons of commercial confidentiality. The Baltic ships, as expected, tend to show inadequate framing strength (see ref.[10] for a discussion of polar/Baltic class alignment). Ships designed to the Canadian requirements often have significant overstrength in the framing. The Russian vessels again have framing weak relative to plating; and again this is an expected trend. The latest MRS rules have changed the balance, though not to the same degree implied here (more general class comparisons are shown in ref. [3]).

Ship number:	4	14	16	21	39	48-50	51	ship 1	ship 2	ship 3	ship 4	SA-15	Samotlor	Oden
BOW REGION														
Class:	1AS	1A	1A	1AS	1A	1AS	1AS	AC4	AC3	AC3	AC4	ULA	UL	Polar 20
Approx Polar Class	6	7	7	6	7	6	6	1	2	2	2	3	5	2
Approx hull form family	2	2	2	2	2	2	2	4.00	4.00	1.00	4.00	5	2.00	4.00
Displacement:	20.8	14.8	8.3	19.7	11.3	22.1	9.6	6.70	5.69	38.94	6.62	25.55	22.52	13.00
Web height	370	298	260	300	250	320	200	230.00	250.00	508.00	375.00	420.00	240.00	900.00
Web thickness (gross)	13.0	11.0	10.0	11.0	9.0	13.0	10.0	38.00	20.00	32.00	35.00	12.00	10.00	28.00
flange width	39	33	100	33	90	39	30	0	0	0	0	122		200
flange thickness (gross)	30	24	20	24	13	26	16	0	0	0	0	12		35
Associated plate thickness (gross)	19.0	19.5	17.0	21.5	17.5	24.0	19.0	41.0	25.4	36.0	35.0	34.0	23	48
Associated plate wide	300	350	350	350	300	350	350	400.0	250.0	305.0	375.0	400.0	700	850
frame span	3.4	1	3	2	3	3	1	0.5	0.5	0.5	1.5	1.3	1.8	4
FY	235	235	235	235	235	235	235	360.0	360.0	360.0	360.0	320.0	240	490
Plate thickness actual:required	1.04	0.99	0.92	1.05	1.08	1.16	1.01	1.24	1.33	1.19	1.30	1.05	0.68	1.05
Shear area actual(g): required (n)	1.06	0.73	0.73	0.66	0.66	0.80	0.53	1.47	1.80	2.21	1.05	0.49	0.24	1.08
Modulus actual (g):required (n)	0.41	1.02	0.44	0.43	0.31	0.52	0.67	4.10	5.42	11.91	1.48	1.09	0.12	1.39

Ship number:	4	14	16	21	39	48-50	51	ship1	ship2	ship3	ship4	SA-15	Samotlor	Oden
MIDBODY														
Web height	300	220	230	280	240	220	200	200.00		400.00		300.00	260.00	500.00
Web thickness (gross)	11.0	10.0	10.0	11.0	12.0	11.0	10.0	35.00		34.00		11.00	11.00	21.00
flange width	33	30	100	33	36	33	30	0		0		0		200
flange thickness (gross)	24	18	10	22	19	18	16	0		0		0		25
Associated plate thickness (gross)	19.0	14.0	13.5	19.5	13.5	17.0	15.5	38.0		32.0		24.5	16	34
Associated plate wide	400	350	350	400	325	343	350	500.0		406.0		400.0	700	850
frame span	3	2	4	2	4	2	2	1.0		1.5		1.3	1.8	3
FY	235	235	235	235	235	235	235	360	360	360	360	320	240	490
Plate thickness actual:required	1.30	1.21	1.25	1.35	1.27	1.29	1.28	1.19		1.09		1.04	0.49	0.96
Shear area actual(g): required (n)	1.54	1.61	2.03	1.47	2.48	1.24	1.39	0.76		1.23		0.53	0.47	1.16
Modulus actual (g):required (n)	0.75	0.77	0.59	1.02	0.49	0.72	0.70	0.78		1.48		0.56		1.27

9. SUMMARY AND CONCLUSIONS

This document has presented the rationale for the use of plastic design for framing, and has shown how a set of design criteria have been developed to allow this. Stress, strain and deflection levels are all important considerations, and all are kept within acceptable limits by the analytical representations of the design point in the draft UR. This has been checked by extensive numerical analysis of frames that comply with the proposed requirements. Large factors of safety against ultimate failure are also assured by additional stability criteria.

Checks have been undertaken to ensure that the proposed requirements are not excessively complex, and that they can be used to develop practical design solutions. Comparisons with existing ships` scantlings show expected trends.

Potential users of these requirements, and other interested parties, are encouraged to use and comment on this system of equations.

REFERENCES

[1] Maritime Register of Shipping Rules for Ice Strengthening of Ships and Icebreakers, October 1999

[2] Transport Canada 'Equivalent Standards for the Construction of Arctic Class Ships' TP 12260, 1995

[3] Background Paper on the IACS Unified Requirements for Polar Class Ships – Class factors and Design Scenarios (tbd)

[4] Background Paper on the IACS Unified Requirements for Polar Class Ships – Load Models (tbd)

[5] 'Ultimate Strength of Laterally Loaded Stifferers' D. Beghin, BV, July 1999 Discussion Paper to IACS Ad-hoc Group

[6] 'Perspectives of Completion of the Discussion on Ice Frames Ultimate Strength' E.Appolonov and A. Nestorov, KSRI , A.Didkovski, MRS September 22, 1999 Discussion Paper to IACS Ad-hoc Group

[7] 'Physical Testing and Finite Element Analysis of Icebreaking Ship Structures in the Post-Yield Region' J. Bond & S. Kennedy, Proceedings of 8th ISOPE, Montreal, 1998

[8] 'Investigation of Plastic Instability in Laterally Loaded Frames' C. Daley, F. Ralph, and H. Sidhu' 4th Canadian Marine Structures and Hydrodynamics Conference, SNAME, Ottawa June 1997

[9] Background Paper on the IACS Unified Requirements for Polar Class Ships – Abrasion and Corrosion (tbd)

[10] 'Alignment of Polar and Baltic Classes' A. Kendrick, AMARK, February 1999 Discussion Paper to IACS Ad-hoc Group

Annex A: Derivation of Section Modulus Requirements for Centered Load
3 Hinge Collapse Case

Introduction

The strength equations in the UR for Polar Ships prescribe required structure to resist the design ice loads. At the design load level the structure is intended to exhibit some plastic behaviour, yet maintaining substantial reserve against actual collapse or rupture. The derivations of strength shown below make use of plastic limit analysis. The load is determined by postulating the formation of a plastic mechanism, and equating internal and external work. The method assumes rigid-plastic material behaviour and ignores large strain and large deflection effects (such as strain hardening and secondary membrane stresses).

This annex derives the nominal plastic strength for a central patch load (fig A.1). At the point of mechanism formation the external work done by the load is equated to the plastic energy absorbed by the structure (per unit displacement).

The normal case involves frames that are built-in on both ends (capable of transmitting a plastic moment to the surrounding structure). For this case we define j=2. Alternate cases of one or zero moment supports we can have j=1 or j=0 (see fig A.2)

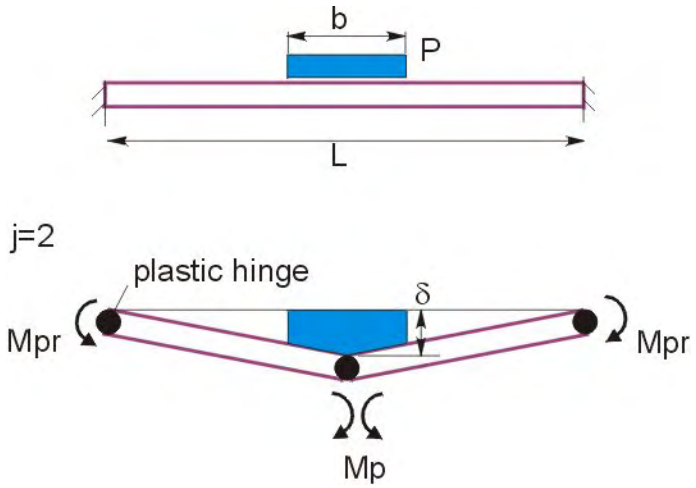

Figure A.1 Sketch of system, with assumed plastic mechanism.

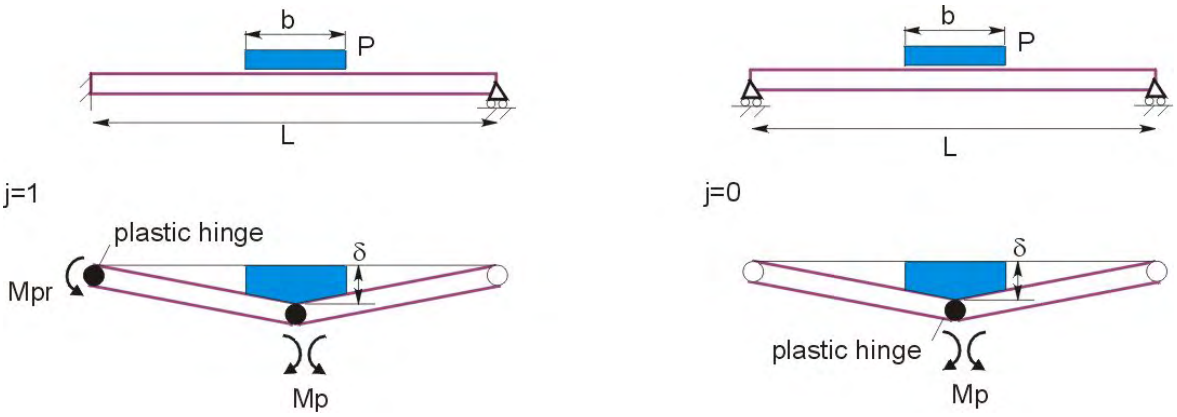

Figure A.2. For 1 or 0 fixed supports (j=1, 0) we continue to assume a centered load, and central hinge.

Energy Balance

We start by balancing internal and external work (see fig A.1Figure). The external work is on the left-hand-side (lhs) of equation (1), and the internal work is on the rhs. The internal work includes the component from the central hinge, unaffected by shear, and the two edge hinges, which have reduced capacity due to shear.

$$(P \cdot b \cdot S)\left(1 - \frac{b}{2 \cdot L}\right) = Mp \cdot \frac{4}{L} + \frac{j}{2} \cdot Mpr \cdot \frac{4}{L} \qquad (1)$$

where:

plastic moment: $Mp = Zp \cdot \sigma_y$ (2)

reduced plastic moment: $Mpr = Zpr \cdot \sigma_y$ (3)

note: j: no of fixed supports
fixed-fixed, j = 2
pinned-fixed, j = 1
pinned-pinned, j = 0

On substitution of (2) and (3) into (1) we have:

$$(P \cdot b \cdot S)\left(1 - \frac{b}{2 \cdot L}\right) = 4 \cdot \frac{\sigma_y}{L} \cdot \left(Zp + \frac{j}{2} \cdot Zpr\right) \qquad (4)$$

The next step is to determine the values of Zp and Zpr, for which there are two alternatives.

Case 1 : Simple Reduced Plastic Modulus

The simplest way to determine the reduced moment capacity is to use a reduced modulus. If we assume a simple quadratic interaction diagram (fig A.3Figure), we can express the reduced modulus in terms of the full modulus and the portion of the shear capacity used.

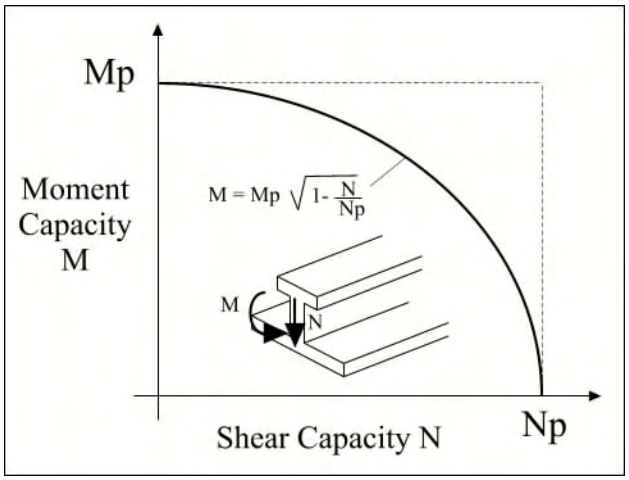

Figure A.3. Assumed simple interaction diagram. The plastic moment and shear combine according to the quadratic interaction.

We can express the reduced modulus as:

$$Zpr = Zp \cdot \sqrt{1 - \left(\frac{\tau}{\tau_y}\right)^2} \tag{5}$$

where

Shear stress in web: $$\tau = \frac{P \cdot b \cdot S}{2 \cdot Aw} \tag{6}$$

Yield shear stress: $$\tau_Y = \frac{\sigma_Y}{\sqrt{3}} \tag{7}$$

The minimum allowable web area *Ao* corresponds to yield under the design load.

$$\tau_y = \frac{P \cdot b \cdot S}{2 \cdot Ao} \tag{8}$$

Solving for Ao:

$$Ao = \frac{1}{2} P \cdot b \cdot S \cdot \frac{\sqrt{3}}{\sigma_y} \tag{9}$$

We can express the reduced modulus (eqn (5)) as:

$$Zpr = Zp \cdot \sqrt{1 - \frac{1}{An^2}} \tag{10}$$

where:

$$An = \frac{Aw}{Ao} \tag{11}$$

We denote the minimum modulus (required if web is fully effective) as:

$$Zo = \frac{P \cdot b \cdot S}{8 \cdot \sigma_y} \cdot \left(1 - \frac{b}{2 \cdot L}\right) \cdot L \tag{12}$$

We can re-write the capacity equation (eqn. (4)) as;

$$2 \cdot Zo = Zp + \frac{j}{2} \cdot Zpr \tag{13}$$

which, using eqn (10), is simplified to:

$$2 \cdot Zo = Zp\left[1 + \frac{j}{2} \cdot \sqrt{1 - \left(\frac{1}{An}\right)^2}\right] \tag{14}$$

Setting the normalized modulus to:

$$Zn = \frac{Zp}{Zo} \tag{15}$$

we get the interaction equation:

$$Zn = \frac{2}{\left[1 + \frac{j}{2} \cdot \sqrt{1 - \left(\frac{1}{An}\right)^2}\right]} \tag{16}$$

Interaction Plot

Equation (17) relates the normalized section modulus (moment capacity) to the normalized web area (shear capacity). The interaction plot shows the minimum combination of section modulus and shear area that will support the load (see fig A.4)

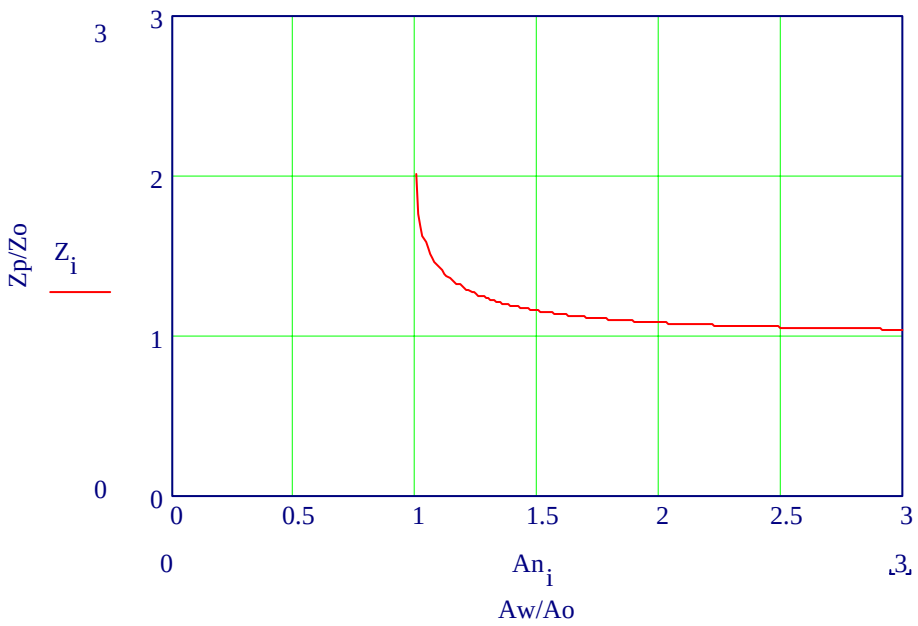

Figure A.4. Interaction plot for moment and shear.

Capacity Equation

We now want to derive the capacity equation for 3 hinge collapse (centered load). This allows us to determine the load, given a particular section. By combining equations (4) (9), (10) we get:

$$(P \cdot b \cdot S) \cdot \left(1 - \frac{b}{2 \cdot L}\right) = 4 \cdot \frac{\sigma_y}{L} \cdot \left[Zp + Zp \cdot \frac{j}{2} \cdot \sqrt{1 - \frac{3}{4} \cdot P^2 \cdot b^2 \cdot \frac{S^2}{Aw^2 \cdot {\sigma_y}^2}} \right] \tag{17}$$

solving for P:

$$P = \frac{1 + \frac{j}{2} \cdot \sqrt{3 \cdot \left(j^2 - 4\right) \cdot Zpns + 1}}{3 \cdot j^2 \cdot Zpns + 1} \cdot Zp \cdot \sigma_y \cdot \frac{4}{(L \cdot b \cdot S) \cdot \left(1 - \frac{b}{2 \cdot L}\right)} \tag{18}$$

where the term *Zpns* (*Zp*-normalized-squared) is:

$$Zpns = \left[\frac{Zp}{Aw \cdot L \cdot \left(1 - \frac{b}{2 \cdot L}\right)} \right]^2 \tag{19}$$

For various values of j the specific solutions are:

$$P_{1h} = 4 \cdot \sigma_y \cdot \frac{Zp}{b \cdot S \cdot L \cdot \left(1 - \frac{b}{2 \cdot L}\right)} \qquad \text{j=0} \qquad (20)$$

$$P_{2h} = 4 \cdot \sigma_y \cdot \frac{Zp}{b \cdot S \cdot L \cdot \left(1 - \frac{b}{2 \cdot L}\right)} \cdot \frac{1 + \frac{1}{2} \cdot \sqrt{1 - 9 \cdot Zpns}}{3 \cdot Zpns + 1} \qquad \text{j=1} \qquad (21)$$

[Note: the pinned-fixed case (P2h) requires that the term under the square root sign is positive. This is equivalent to the requirement that the structure does not collapse by shear at both supports. For *9xZpns* to be less than 1, P1h must be less than 1.155 x P2s.]

$$P_{3h} = 4 \cdot \sigma_y \cdot \frac{Zp}{b \cdot S \cdot L \cdot \left(1 - \frac{b}{2 \cdot L}\right)} \cdot \frac{1}{6 \cdot Zpns + \frac{1}{2}} \qquad \text{j=2} \qquad (22)$$

Summary - Case 1: Simple Reduced Plastic Modulus

This completes the derivation of the strength requirements for a centered load for the case of a simple shear-bending interaction. The interaction diagram is given by Equation (16), and the capacity is given by Equation (18) (or variants (20), (21), (22)). This case results in a complete loss of bending capacity when the web is fully yielded. This approach does not take into account the contribution of the flanges to either bending or shear after the web is fully yielded.

In the next section we will make the assumption that the shear will only affect the contribution of the web to the bending moment.

Case 2: Reduced Plastic Modulus Using Web Stress

We now examine the case in which the modulus is only reduced by the loss of web capacity.

The section modulus (assuming PNA is at the web/plate connection) is:

$$Zp = Zf + Zw \tag{23}$$

where:

$$Zf = Af \cdot \left(\frac{tf}{2} + hw + \frac{tp}{2} \right) \tag{24}$$

$$Zw = Aw \cdot \left(\frac{hw}{2} + \frac{tp}{2} \right) \tag{25}$$

This results in :

$$Zp = Af \cdot \left(\frac{tf}{2} + hw + \frac{tp}{2} \right) + Aw \cdot \left(\frac{hw}{2} + \frac{tp}{2} \right) \tag{26}$$

We again start by balancing internal and external work:

$$(P \cdot b \cdot S) \cdot \left(1 - \frac{b}{2 \cdot L} \right) = Mp \cdot \frac{4}{L} + \frac{j}{2} \cdot Mpr \cdot \frac{4}{L} \tag{27}$$

where:

$$Mp = Zp \cdot \sigma_y \tag{28}$$

$$Mpr = Zpr \cdot \sigma_y \tag{29}$$

which again gives

$$(P \cdot b \cdot S) \cdot \left(1 - \frac{b}{2 \cdot L} \right) = 4 \cdot \frac{\sigma_y}{L} \left(Zp \cdot + \frac{j}{2} \cdot Zpr \right) \tag{30}$$

The shear is assumed to affect only the web's ability to contribute to bending. The reduced capacity is therefore given by:

$$Zpr = Zf + Zw \cdot \sqrt{1 - \left(\frac{\tau}{\tau_y} \right)^2} \tag{31}$$

which can be stated as:

$$Zpr = Zp \cdot \left[1 - kw \cdot \left[1 - \sqrt{1 - \left(\frac{Ao}{Aw} \right)^2} \right] \right] \tag{32}$$

where:

$$kw = \frac{Zw}{Zp} \tag{33}$$

an approximate (within a few %) value for kw is :

$$kw = \frac{1}{1 + 2 \cdot \frac{Af}{Aw}} \quad \text{(approx)} \tag{34}$$

using equations (11), (12), (15), (30), and (32) the interaction equation can be written as:

$$Zn = \frac{2}{\left[1 + \frac{j}{2} + kw \cdot \frac{j}{2} \cdot \left[\sqrt{1 - \left(\frac{1}{An} \right)^2} - 1 \right] \right]} \tag{35}$$

the required modulus is:

$$Zp = \frac{Zo \cdot 2}{\left[1 + \frac{j}{2} + kw \cdot \frac{j}{2} \cdot \left[\sqrt{1 - \left(\frac{1}{An} \right)^2} - 1 \right] \right]} \tag{36}$$

where *Zo* and *Ao* are given by equations (9) and (12). Equation (35) is similar to (16), with the addition of a *kw* term. Using Equation (34) we plot the interaction equation for various *Af/Aw* ratios (see fig A.5).

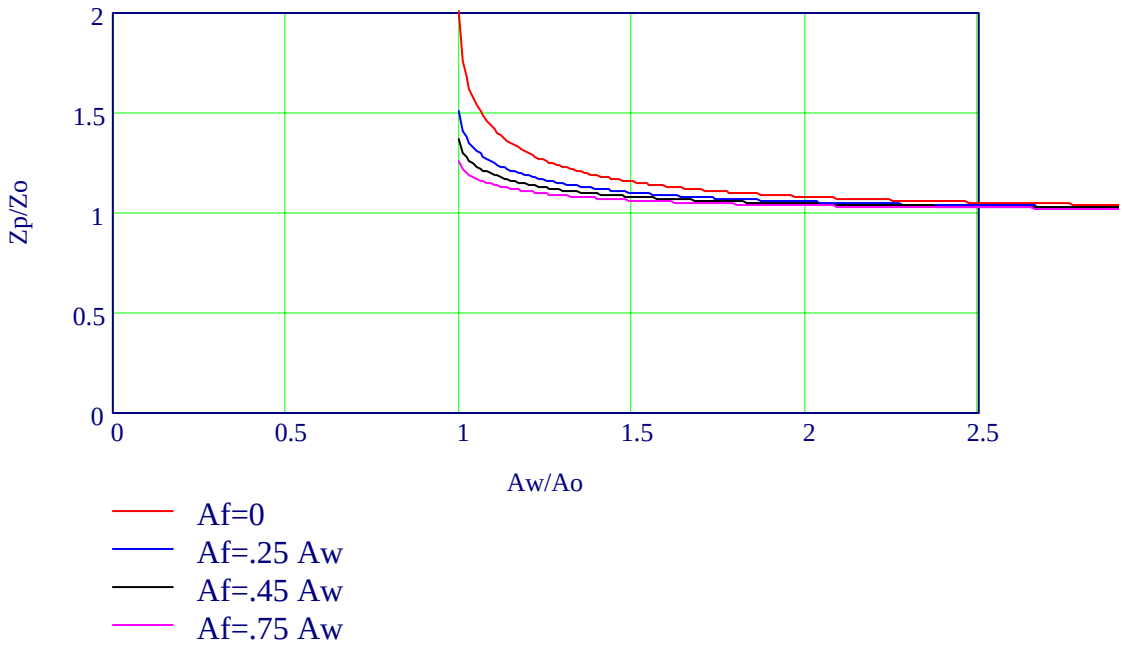

Figure A.5. Interaction plot for moment and shear.

Capacity Equation

We again want to derive the capacity equation for 3 hinge collapse (centered load). combining equations (9), (33), (35) gives:

$$(P\cdot b\cdot S)\left(1-\frac{b}{2\cdot L}\right)=4\cdot\frac{\sigma_y}{L}\cdot Zp\cdot\left[\frac{j}{2}+1+kw\cdot\frac{j}{2}\cdot\left[\sqrt{1-\left[\frac{\frac{1}{2}\cdot P\cdot b\cdot S\cdot\frac{\sqrt{3}}{\sigma_y}}{Aw}\right]^2}-1\right]\right] \tag{37}$$

solving for P:

$$P=\frac{\left[j+2-kw\cdot j+kw\cdot j\cdot\sqrt{1+3\cdot(j+2)\cdot Zpns\cdot(-j+2\cdot kw\cdot j-2)}\right]}{6\cdot Zpns\cdot kw^2\cdot j^2+2}\cdot\sigma_y\cdot Zp\cdot\frac{4}{\left[b\cdot S\cdot L\cdot\left(1-\frac{b}{2\cdot L}\right)\right]} \tag{38}$$

where *Zpns* is defined in equation (19)

for j=0 (0 fixed supports) solving for P, we have the pressure to cause collapse

$$P_{1h} = 4 \cdot \sigma_y \cdot \frac{Zp}{\left[b \cdot S \cdot L \cdot \left(1 - \frac{b}{2 \cdot L} \right) \right]} \qquad j=0 \quad (39) \text{ (same as 20)}$$

for j=1 (1 fixed support) solving for P, we have the pressure to cause collapse

$$P_{2h} = \frac{(3 - kw) + kw \cdot \sqrt{1 + 9 \cdot Zpns \cdot (2 \cdot kw - 3)}}{2 \cdot \left(3 \cdot Zpns \cdot kw^2 + 1 \right)} \cdot Zp \cdot \sigma_y \cdot \frac{4}{(S \cdot b \cdot L) \cdot \left(1 - \frac{b}{2 \cdot L} \right)} \qquad j=1 \quad (40)$$

for j=2, solving for P, we have the pressure to cause 3 hinge collapse:

$$P_{3h} = \frac{(2 - kw) + kw \cdot \sqrt{1 - 48 \cdot Zpns \cdot (1 - kw)}}{12 \cdot Zpns \cdot kw^2 + 1} \cdot \frac{Zp \cdot \sigma_y \cdot 4}{\left[S \cdot b \cdot L \cdot \left(1 - \frac{b}{2 \cdot L} \right) \right]} \qquad j=2 \quad (41)$$

for the term under the root sign to stay positive, Zp must be less than Zpmax, where;

$$Zpmax = \sqrt{\frac{1}{48 \cdot (1 - kw)}} \cdot Aw \cdot L \cdot \left(1 - \frac{b}{2 \cdot L} \right) \qquad (42)$$

note: in cases in which Zp > Zpmax, the frame will first fail by shear at both supports (central load). In this case the capacity is nominally limited by:

$$Plim = 2 \cdot \frac{Aw \cdot \sigma_y}{\sqrt{3} \cdot S \cdot b} \qquad (43)$$

Comparison with plastic FE analysis

Two frames were analyzed using non-linear finite element analysis. In both cases a patch load was applied in the center. The frames are shown in fig A.6:

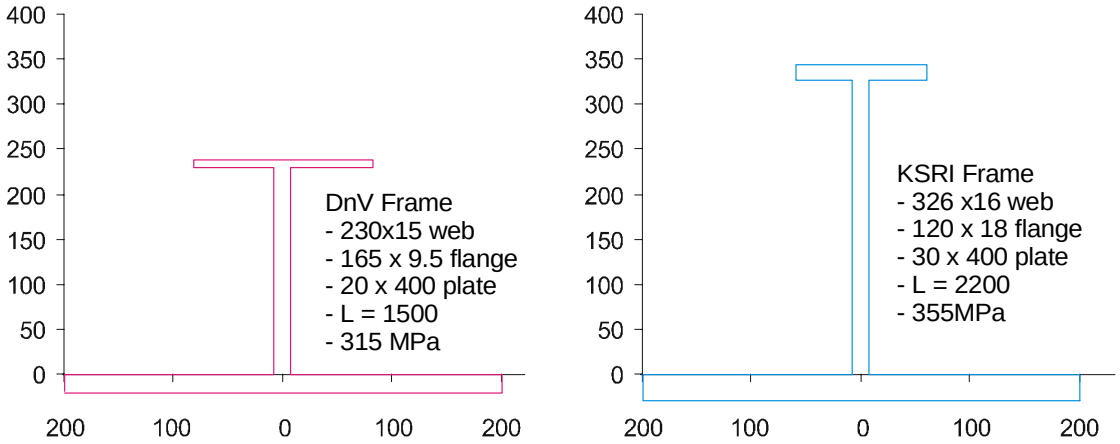

Figure A.6. Frames used in validation exercise.

The FE load-deflection curves and the values calculated from equation (41) are shown below (see fig A.7). Also shown are the results of equation (22). The calculated values agree very well with the onset of large permanent deformations. Equation (41) allows higher pressures, and yet is still conservative.

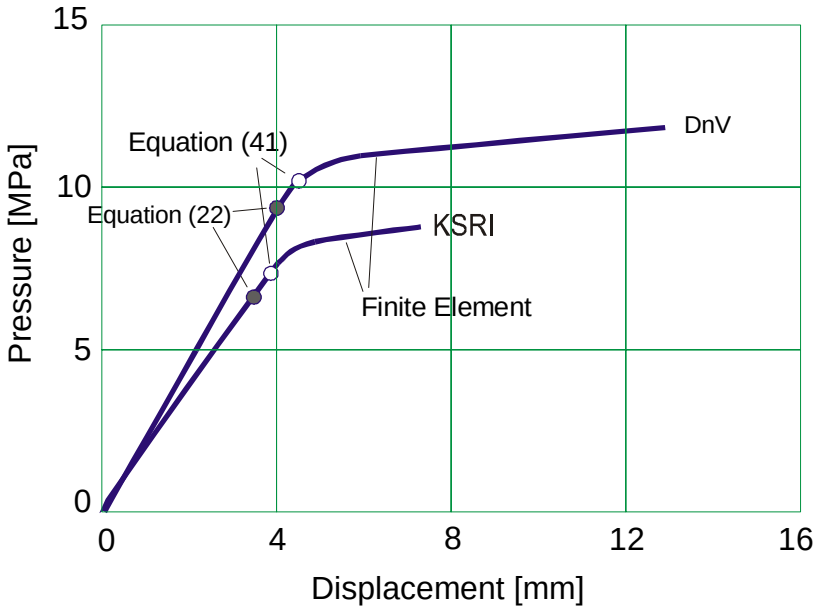

FigureA.7. Comparison of equations with finite-element results.
note: the DnV pressure was applied over 300 mm, while the
KSRI pressure was applied over 710 mm.

Rule equations

The above derivations lead to two possibilities for a rule equation for checking symmetrical loads. Both start with equation (9) for minimum shear area Ao, (which was defined ***Am*** (eqn 9.1) in the may'99 draft of the UR):

$$Ao = \frac{1}{2} \cdot P \cdot b \cdot S \cdot \frac{\sqrt{3}}{\sigma_y} \tag{9}$$

The may'99 draft of the UR contained a rule formula for required section modulus *Zp*, equivalent to equation (17), which with slight re-arrangement can be written as (identical to **(Zpm)min** (eqn 9.1) in the may'99 UR):

$$Zp = \frac{(P \cdot b \cdot S \cdot L)}{4 \cdot \sigma_y} \cdot \left(1 - \frac{b}{2 \cdot L}\right) \cdot A1 \tag{44}$$

where:

$$A1 = \frac{1}{\left[1 + \frac{j}{2} \cdot \sqrt{1 - \left(\frac{Ao}{Aw}\right)^2}\right]} \tag{45}$$

New Formula

An improved formula can be found by by re-arranging (36). This proposed formula for *Zp*, would replace **(Zpm)min** (eqn 9.1) in the may'99 UR.

$$Zp = \frac{(P \cdot b \cdot S \cdot L)}{4 \cdot \sigma_y} \cdot \left(1 - \frac{b}{2 \cdot L}\right) \cdot A2 \tag{46}$$

$$A2 = \frac{1}{1 + \frac{j}{2} + \frac{j}{2} \cdot kw \cdot \left[\sqrt{1 - \left(\frac{Ao}{Aw}\right)^2} - 1\right]} \tag{47}$$

where:

$$kw = \frac{1}{1 + 2 \cdot \frac{Af}{Aw}}$$

Annex B: Derivation of Section Requirements for Off-center Load Shear Hinge Collapse Case

Introduction

The strength equations in the UR for Polar Ships prescribe required structure to resist the design ice loads. At the design load level the structure is intended to exhibit some plastic behaviour, yet maintaining substantial reserve against actual collapse or rupture. The derivations of strength shown below make use of plastic limit analysis. The load is determined by postulating the formation of a plastic mechanism, and equating internal and external work. The method assumes rigid-plastic material behaviour and ignores large strain and large deflection effects (such as strain hardening and secondary membrane stresses).

This annex derives the nominal plastic strength for an off-center (asymmetrical) patch load (see fig B.1). At the point of mechanism formation the external work done by the load is equated to the plastic energy absorbed by the structure (per unit displacement).

The normal case involves frames that are built-in on both ends (capable of transmitting a plastic moment to the surrounding structure). This case will only be considered for both ends fixed (j=2). In the case of j=1 (far end pinned) the solution results in a value of 'a' greater than L/2, and is thus illogical. Practically, this means that we only check this mechanism for j=2, and that pinned connections are not to be allowed in the ice-strengthened areas.

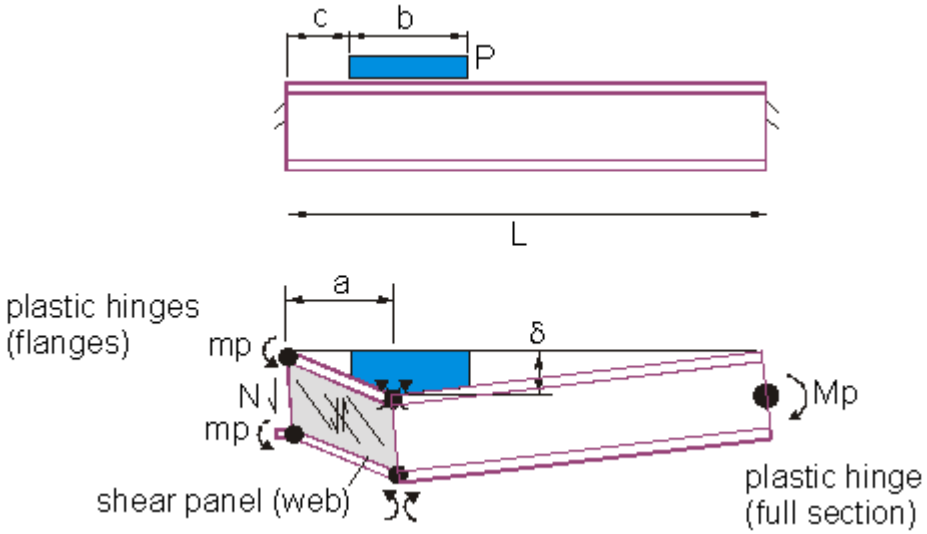

Figure B.1. sketch of system, with assumed plastic mechanism :

Energy Balance

The external work done is found by integrating the external load over the deformation (for δ =1). The general equation (see fig B.2) for the external work (*EWD*) is;

$$EWD = P \cdot S \frac{(a-c)\left(\frac{1}{2}(c+a)\right)}{a} + \frac{(b+c-a)\left(L-\frac{1}{2}(a+b+c)\right)}{L-a} \tag{1}$$

We can simplify this by finding the location (value of *c*) which maximizes the work done. This is done by using;

$$\frac{\partial}{\partial c} EWD = 0 \tag{2}$$

When solving the above for *c* we get;

$$c = a \cdot \left(1 - \frac{b}{L}\right) \tag{3}$$

Substituting (3) into (1) , we get;

$$EWD = P \cdot b \cdot S \cdot \left(1 - \frac{b}{L}\right) \tag{4}$$

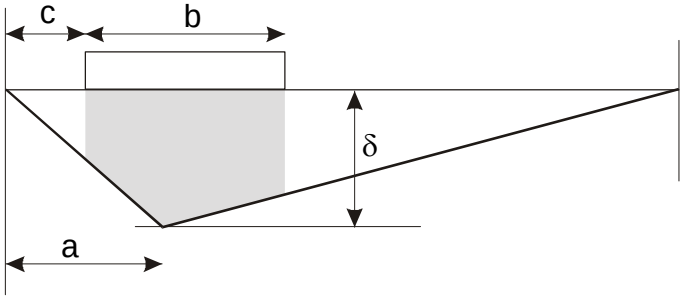

Figure B.2. Shape of asymmetrical collapse.

The internal work (IWD) per unit deflection includes the plastic work done by the shear panel, the 4 small plastic hinges in the flanges and the large plastic hinge at the far end. The equation is;

$$IWD = N + \frac{Mp}{L-a} + mp \cdot \left(\frac{2}{a} - \frac{1}{L-a}\right) \tag{5}$$

where:

shear force in web: $$N = Aw \cdot \frac{\sigma_y}{\sqrt{3}} \quad (6)$$

plastic moment in full frame: $$Mp = Zp \cdot \sigma_y \quad (7)$$

sum of local plastic moments in plate and flange: $$mp = zp \cdot \sigma_y \quad (8)$$

sum of local plastic section mod. $$zp = zp_{plate} + zp_{flange} \quad (9)$$

local plastic section modulus of shell plate $$zp_{plate} = S \cdot \frac{tp^2}{4} \quad (10)$$

local plastic section modulus of flange $$zp_{flange} = wf \cdot \frac{tf^2}{4} \quad (11)$$

section modulus of frame (assumes NA at plate/web join) $$Zp = Af \cdot \left(\frac{tf}{2} + hw + \frac{tp}{2} \right) + Aw \cdot \left(\frac{hw}{2} + \frac{tp}{2} \right) \quad (12)$$

Equating EWD with IWD gives an energy balance equation of :

$$(P \cdot b \cdot S)\left(1 - \frac{b}{2 \cdot L}\right) = \sigma_y \cdot \left[\frac{Aw}{\sqrt{3}} + Zp \cdot \left[\frac{1}{L-a} + kz \cdot \left(\frac{2}{a} - \frac{1}{L-a} \right) \right] \right] \quad (13)$$

where:

ratio of local to total moduli $$kz = \frac{zp}{Zp} \quad (14)$$

The value of a will be that which minimizes the internal work. This is found by taking the derivative of IWD with respect to '*a*' and setting it to zero. This gives;

$$\frac{d}{da}\left[\frac{1}{L-a} + kz \cdot \left(\frac{2}{a} - \frac{1}{L-a} \right) \right] = 0 \quad (15)$$

Solving (15) for a/L, we get;

$$\frac{a}{L} = \frac{1}{2\cdot(kz-1)}\cdot\left[4\cdot kz - 2\cdot\sqrt{2\cdot kz^2 + 2\cdot kz}\right] \qquad \underline{\text{exact}} \quad (16)$$

This is the exact solution. An approximate solution is;

$$\frac{a}{L} = .64\cdot kz^{.3333} \qquad \underline{\text{approximate}} \quad (17)$$

When we plot the two equations, we see that (17) is a very good approximation to (16). Note that *a/L* is only a function of *kz*, so this comparison will hold for all cases.

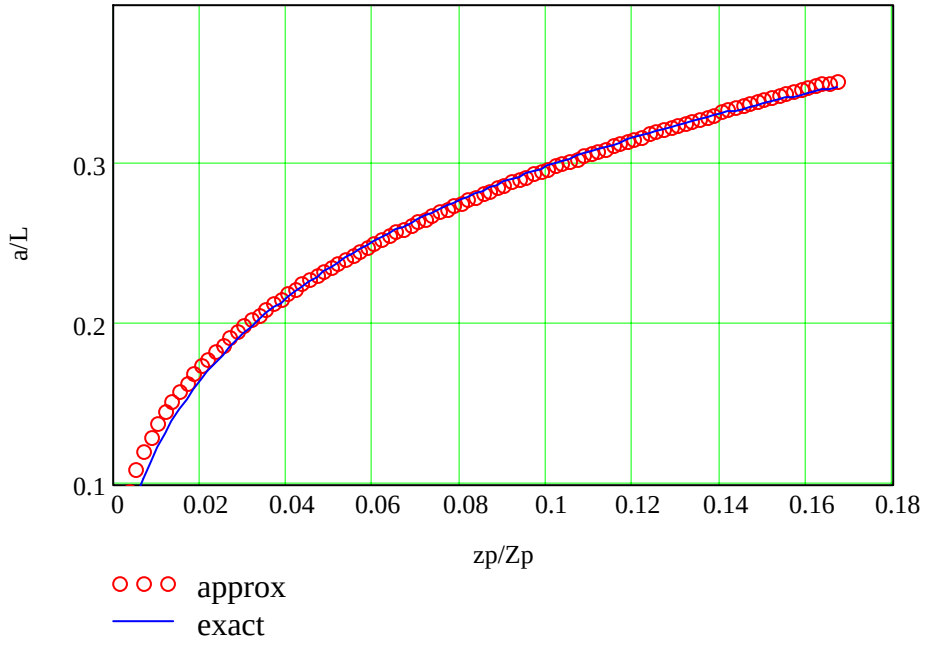

Figure B.3. Comparison of exact and approximate values of *a/L*

Now, we can write the energy equation as;

$$(P\cdot b\cdot S)\left(1-\frac{b}{2\cdot L}\right) = \sigma_y\cdot\left[\frac{Aw}{\sqrt{3}} + \frac{Zp}{L}\cdot fz\right] \qquad (18)$$

where *fz* depends on *a/L* and *kz*. *fz* can be expressed as exactly (substituting (16) into (13) and solving exactly), near-exact (substituting (17) into (13) and solving exactly) or approximately (fitting the exact solution to a simpler equation)). The exact solution for *fz* is:

$$fz = \frac{-(kz-1)^2\cdot\sqrt{2}\cdot\sqrt{kz^2+kz}}{\left(\sqrt{2}\sqrt{kz^2+kz}-2\cdot kz\right)\cdot\left(\sqrt{2}\sqrt{kz^2+kz}-kz-1\right)} \qquad (19)$$

The near-exact solution is (uses approx *a/L*);

$$fz = \frac{1}{1-.64\cdot kz^{.3333}} + kz\cdot\left(\frac{2}{.64\cdot kz^{.3333}} + \frac{1}{1-.64\cdot kz^{.3333}}\right) \tag{20}$$

The approximate solution for *fz* is;

$$fz = 1.1 + 5.75\cdot kz^{.7} \tag{21}$$

Equations (19), (20), (21) are plotted in Figure. The plot shows that all 3 equations are equivalent (<1% error). Again, as *fz* is only a function of *kz*, this comparison will be the same for all cases.

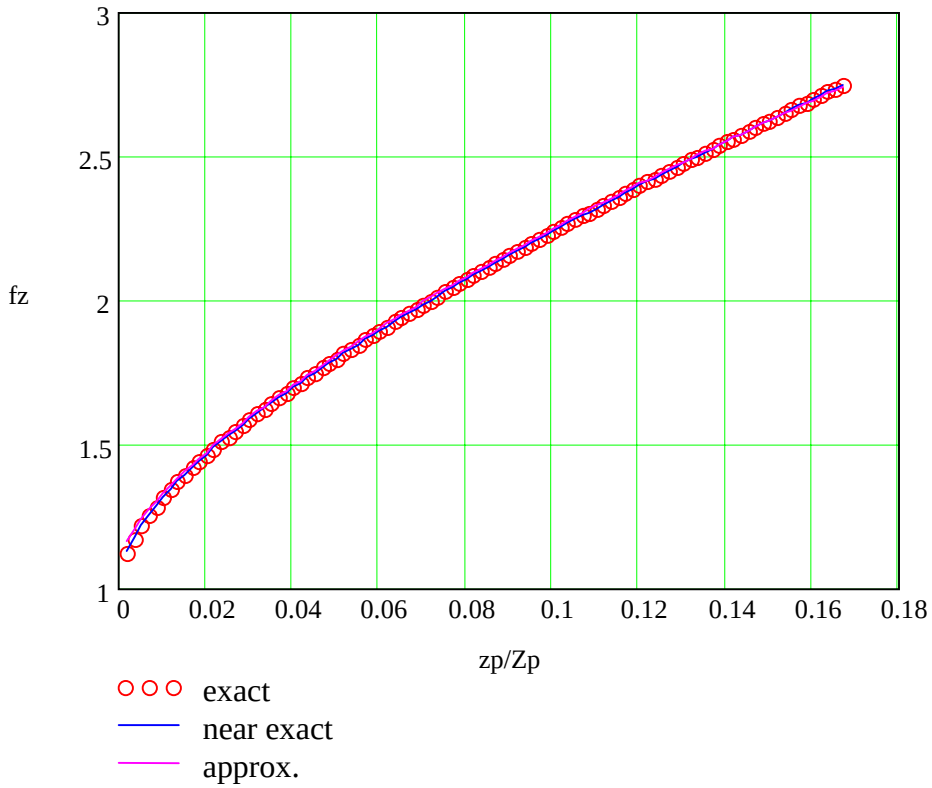

Figure B.4. Comparison of formulae for fz.

The above derivations have enabled us to develop a relatively simple energy equation, which accounts for the optimal load and hinge locations. Figure shows that the simplifications have not diminished the accuracy of the solution. We can write the energy balance equation in the simple form;

$$(P \cdot b \cdot S)\left(1-\frac{b}{2 \cdot L}\right)=\sigma_y \cdot\left[\frac{Aw}{\sqrt{3}}+\frac{Zp}{L} \cdot (1.1+5.75 \cdot kz^{.7})\right] \tag{22}$$

We now wish to cast this equation in a non-dimensional form, compatible with the form of the interaction equations for the 3-hinge case. Equation (22) can be re-written as;

$$1=\frac{Aw}{(P \cdot b \cdot S)\left(1-\frac{b}{2 \cdot L}\right) \cdot \frac{\sqrt{3}}{\sigma_y}}+\frac{Zp}{(P \cdot b \cdot S)\left(1-\frac{b}{2 \cdot L}\right) \cdot \frac{L}{\sigma_y}} \cdot (1.1+5.75 \cdot kz^{.7}) \tag{23}$$

As in the case of 3 hinge , we define the minimum web area Ao:

$$Ao=\frac{1}{2} P \cdot b \cdot S \cdot \frac{\sqrt{3}}{\sigma_y} \tag{24}$$

We denote the minimum modulus as:

$$Zo=\frac{P \cdot b \cdot S}{8 \cdot \sigma_y}\left(1-\frac{b}{2 \cdot L}\right) \cdot L \tag{25}$$

Using *Ao* and *Zo*, we can re-write the capacity equation as:

$$1=\frac{Aw}{2 \cdot\left(1-\frac{b}{2 \cdot L}\right) \cdot Ao}+\frac{Zp}{8 \cdot Zo} \cdot (1.1+5.75 \cdot kz^{.7}) \tag{26}$$

which is simplified to:

$$1=\frac{An}{2 \cdot\left(1-\frac{b}{2 \cdot L}\right)}+\frac{Zn}{8} \cdot (1.1+5.75 \cdot kz^{.7}) \tag{27}$$

where *Zn* and *An* are normalized values;

Normalized modulus $$Zn=\frac{Zp}{Zo} \tag{28}$$

Normalized web area $$An=\frac{Aw}{Ao} \tag{29}$$

By re-arranging (27), we get the interaction equation;

$$Zn = \frac{8}{(1.1 + 5.75 \cdot kz^{.7})} \cdot \left[1 - \frac{An}{2 \cdot \left(1 - \frac{b}{2 \cdot L} \right)} \right] \tag{30}$$

This interaction equation is a straight line. The *y* intercept is defined as *Zmax*, and the *x* intercept is *Amax*. The equation can be written as;

$$Zn = Z\max \cdot \left(1 - \frac{An}{A\max} \right) \tag{31}$$

where:

Maximum modulus $$Z\max = \frac{8}{(1.1 + 5.75 \cdot kz^{.7})} \tag{32}$$

Maximum web area $$A\max = 2 \cdot \left(1 - \frac{b}{2 \cdot L} \right) \tag{33}$$

Note that the interaction diagram depends on *Amax* (which depends only on the patch/span ratio b/L) and *Zmax* (which depends only on the modulus ratio *kz=zp/Zp*). This allows us to add a *kz* axis to the *y* axis, and a *b/L* axis to the *x* axis.

This interaction equation (31), shows some interesting properties. The equation is linear, meaning that an increase in web area will result in a constant decrease in the section modulus requirement. Two extreme cases (neither actually possible) involve a shear area of Amax, with zero modulus, or a section modulus of Zmax with zero web area. In the first case the entire load would be carried by the web (the plastic shear panel, with no load transmitted to the far end). At the other extreme, with no shear capacity, all the load would be carried by the far end, as a plastic cantilever beam. For all realistic cases the load is carried in three parts; the web to the near end, the flanges to the near end, and the full frame to the far end. A trade-off among the web, flanges and full modulus allow for various possible designs.

Interaction Plot

Interaction plot for shear is illustrated in figure B.5. Nine cases are illustrated to show the range of possible interaction equations for the shear mechanism. This plot would need to be combined with the 3-hinge (central load) interaction diagram to see the effects. The three hinge case will require Aw/Ao and Zp/Zp to both be greater than one. Two example 3-hinge interaction curves are shown (a flat bar and a typical flanged frame). It is clear that there will be cases in which the shear mechanism will never govern. In the case where the load length covers most or all of the frame (b/L ~1), the shear curve will always lie below the 3-hinge curves. In the case of a very concentrated load, especially on a frame with small flanges, shear collapse will more likely govern.

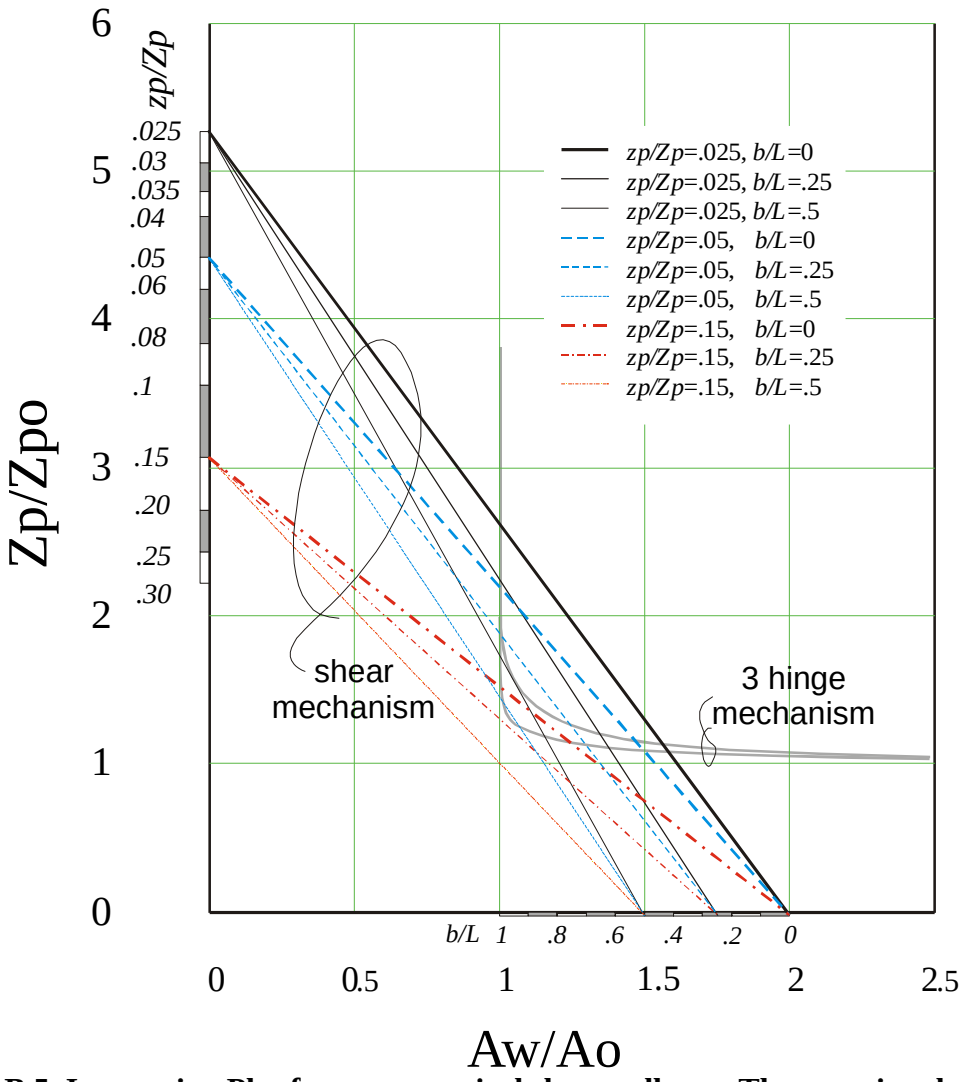

Figure B.5. Interaction Plot for asymmetrical shear collapse. The equation depends on the load patch length and on the ratio zp/Zp.

The capacity equation is just a re-arrangement of (22);

$$P = \frac{\sigma_y}{b \cdot S\left(1 - \frac{b}{2 \cdot L}\right)} \cdot \left[\frac{Aw}{\sqrt{3}} + \frac{Zp}{L} \cdot (1.1 + 5.75 \cdot kz^{.7})\right] \qquad (34)$$

Comparison with plastic FE analysis

Two frames were analyses using non-linear finite element analysis. In both cases the patch load was applied near the edge:

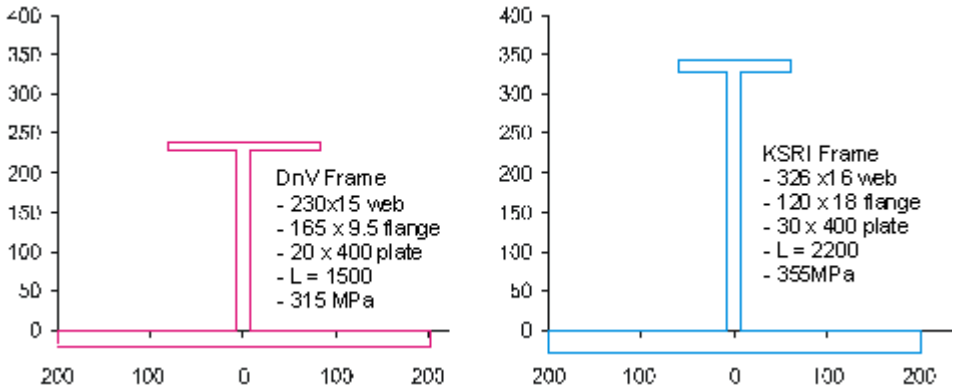

Figure B.6. Frames used for validation exercise.

The FE load-deflection curves and the values calculated from equation (34) are shown below. The calculated values agree very well with the onset of large permanent deformations. For the 'DnV Frame' pressure was applied over 300 mm, while for the 'KSRI Frame' the pressure was applied over 710 mm. It is also important to note that the DnV patch was 100 mm away from the boundary, while the KSRI load was at the boundary. It is likely that the KSRI values would have been a bit lower, had the patch been placed 100mm away from the support.

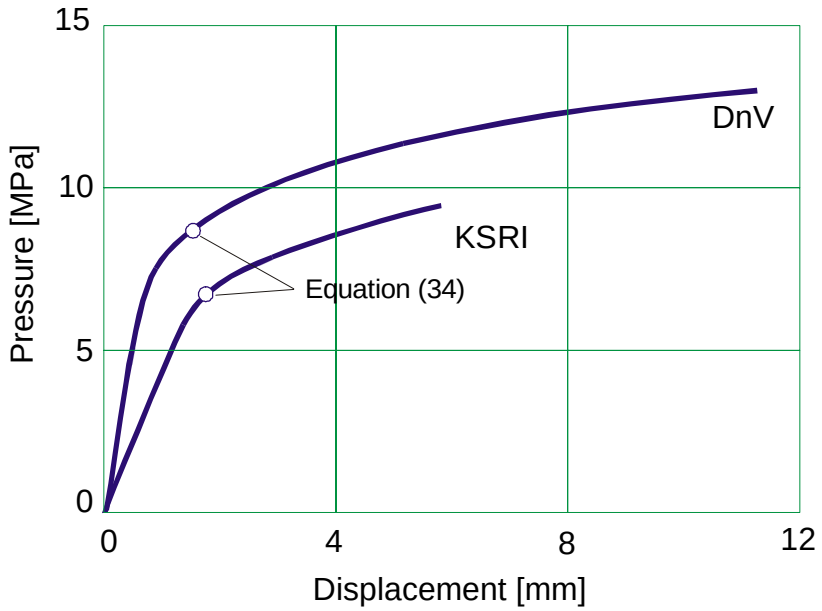

Figure B.7. Comparison of equations with finite element results.

Rule Equations

The above formulations lead to a rule to check that adequate capacity exists to prent shear collapse with an asymmetrical load. By re-arranging (30) we have an additional formula for *Zp*, to augment the central load case in the UR

$$Zp = \frac{P \cdot b \cdot S \cdot L}{4 \cdot \sigma_y} \cdot \left(1 - \frac{b}{2 \cdot L}\right) \cdot A3 \tag{35}$$

where:

$$A3 = \frac{\left[1 - \frac{Aw}{2 \cdot Ao \cdot \left(1 - \frac{b}{2 \cdot L}\right)}\right]}{(.275 + 1.438 \cdot kz^{.7})} \tag{36}$$

$$\mathrm{kz} = \frac{\mathrm{zp}}{\mathrm{Zp}} \tag{14}$$

Annex C: Plastic Frame Capacity using FEA for Polar Shipping Rule Development

Introduction

The IACS Polar Shipping Rule Requirements (IUR) make use of plastic behaviour and plastic section properties for framing. As one aspect of the verification of the rules, a number of non-linear finite element analyses of the plastic behaviour of frames have been conducted. Several sets of analysis have been conducted. For each set the load deflection curves are shown. The symmetric and asymmetric load cases are compared. All frames were modeled with fixed ends, and with symmetric boundary conditions on the long edges (as if the load patch covered several frames identically). As a point of comparison, the pressure required to cause first yield is included in several cases. The yield pressure was determined from the finite element analysis.

Set 1

Table 1 shows the load and geometric parameters for the first set of frames. These frames are nominally similar and approximately suitable for a 20 kT, PC6 in the bow region. The frames have the same shell plate, frame spacing and load height. The web and flange configuration varies. (see the excel spreadsheets for the design calculations for these frames). The term **ps** refers to the calculated shear capacity (in MPa)

The following shows the load-deflection behaviour for 4 frames. The frame parameters are given in Table 1. The shapes are sketched in Figure 1. Figures 2 - 5 give the load deflection curves for the frames.

Table C1. Parameters of frames in Set 1

var	var	F4	F5	F6	F7
load height [mm]	b	928	928	928	928
web height [mm]	hw	402.00	463.00	481.00	494.00
web thk. [mm]	tw	15.42	14.19	14.74	15.16
width of fl. [mm]	wf	46.3	85.1	88.4	90.9
fl. thk. [mm]	tf	15.42	17.02	17.69	18.19
plate thk. [mm]	tp	20.5	20.5	20.5	20.5
fr. spac. [mm]	S	350	350	350	350
fr. span [mm]	lf	2000	2500	3000	3500
fy [MPa]	fy	235	235	235	235
τ_y [MPa]	ty	136	136	136	136
shear [MPa]	**ps**	**4.53**	**4.55**	**4.54**	**4.53**
3 hinge [MPa]	**p3h**	**4.67**	**5.07**	**4.89**	**4.59**

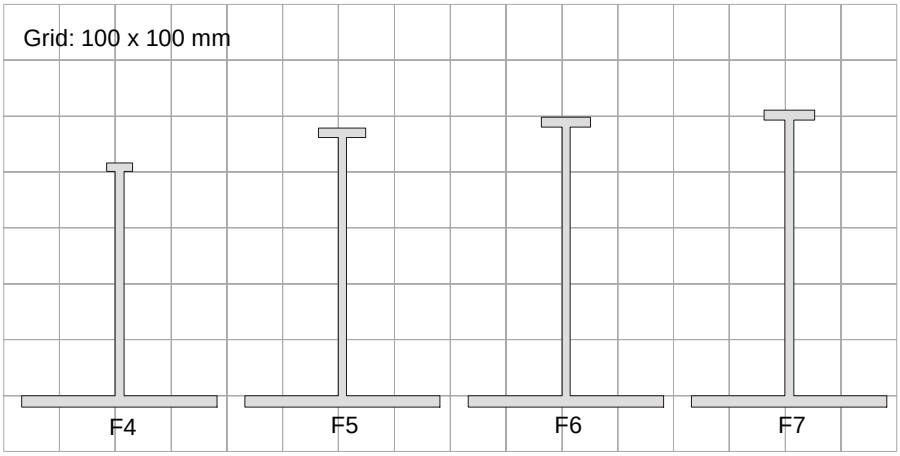

Figure C1. X-sections of the 4 frames in Set 1.

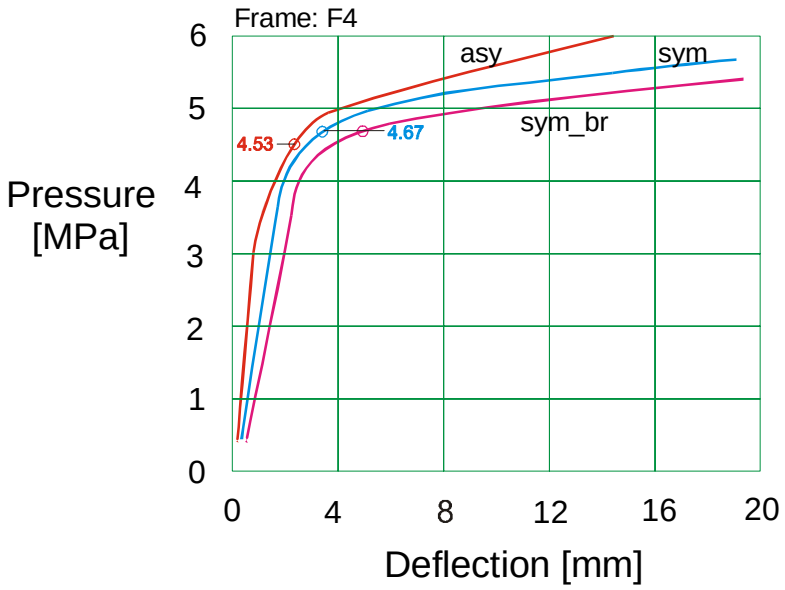

Figure C2 Load-deflection curves for frame F4

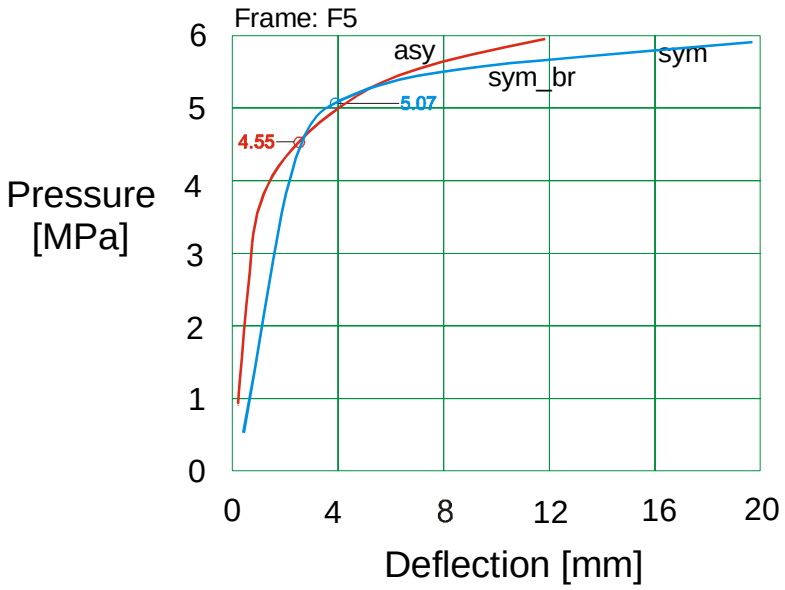

Figure C3 Load-deflection curves for frame F5

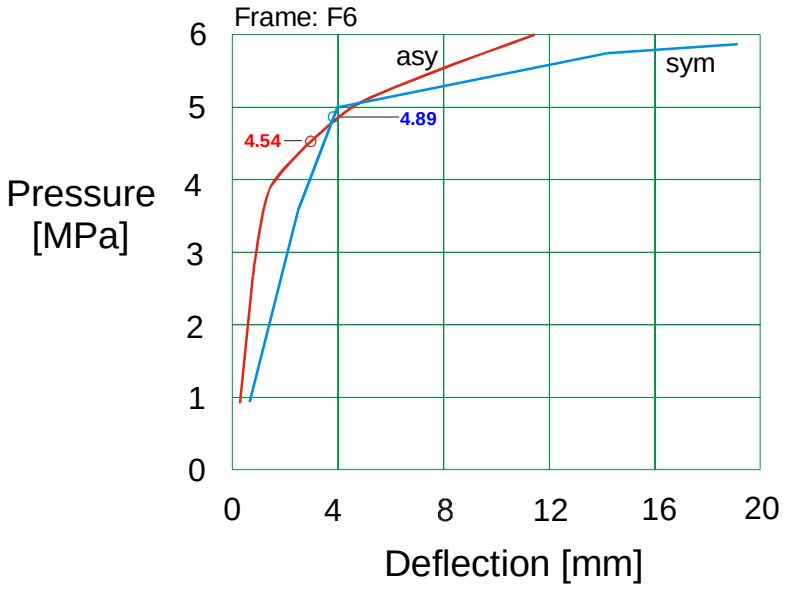

Figure 4 Load-deflection curves for frame F6

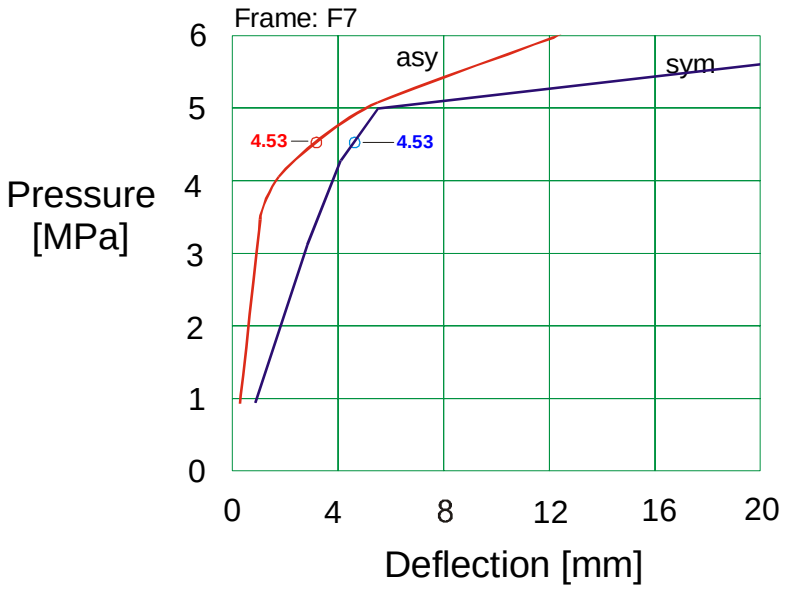

Figure 5 Load-deflection curves for frame F7

Set 2

Tables 2 and 3 shows the load and geometric parameters for the second set of frames. These frames were developed to be suitable for a 30 kT, for all 7 classes in the bow region. (see the excel spreadsheets for the design calculations for these frames). The term **ps** refers to the calculated shear capacity (in MPa). The shapes are sketched in Figure 6. Figures 7,8, 9, 10 give the load deflection curves for four of the frames. Results are presented for the 4 cases highlighted in bold in Tables 2,3.

Table 2. Parameters of frames in Set 2 (bow)

30kT, Bow

var \class	C1 (PC1)	C2 (PC2)	C3 (PC3)	C4 (PC4)	**C4a (PC4)**	C5 (PC5)	C6 (PC6)	**C7 (PC7)**
b [mm]	1220	1180	1120	1060	**960**	1010	1110	**1000**
hw [mm]	620.8	547.3	511.8	484.1	**409.9**	444.3	411.6	**345.3**
tw [mm]	37.5	37.8	21.1	15.8	**21.6**	13	11.3	**10.2**
wf [mm]	187.3	138.8	147.8	142.3	**108.1**	142.8	124.1	**143.2**
tf [mm]	31.8	31.9	27.5	22.9	**21.6**	22.1	20.3	**19.9**
tp [mm]	37.5	30.8	26.4	22.6	**21.6**	20.0	17.4	**15.7**
S [mm]	350	350	350	350	**350**	350	350	**350**
lf [mm]	2500	2500	2500	2500	**3250**	2500	2500	**2500**
fy [MPa]	355	355	355	355	**355**	355	355	**355**
ty [MPa]	205	205	205	205	**205**	205	205	**205**
ps [MPa]	**20.94**	**18.00**	**10.48**	**7.79**	**7.88**	**6.21**	**4.56**	**3.83**
p3h [MPa]	**22.32**	**19.47**	**10.55**	**7.98**	**7.61**	**6.44**	**4.72**	**4.04**

Table 3. Parameters of frames in Set 2 (mid)

30kT, Mid

var	C1	C2	C3	C4	***C4a***	C5	C6	**C7**
b	1040	1000	950	900	***820***	860	940	**820**
hw	444.6	377.6	325.4	308.4	***379.6***	270.1	236.9	**190.8**
tw	30.5	21.7	15.2	11.4	***10.9***	8.9	7.3	**6.5**
wf	152.4	108.7	106.4	102.3	***72.7***	97.8	80.8	**91.4**
tf	25.9	25	19.8	16.5	***16.3***	15.1	13.2	**12.7**
tp	30.5	24.1	19	16.2	***15.5***	13.7	11.3	**10**
S	350	350	350	350	***350***	350	350	**350**
lf	2500	2500	2500	2500	***3250***	2500	2500	**2500**
fy	355	355	355	355	***355***	355	355	**355**
ty	205	205	205	205	***205***	205	205	**205**
ps	**13.12**	**8.08**	**5.06**	**3.75**	***4.21***	**2.66**	**1.74**	**1.41**
p3h	**14.47**	**8.83**	**5.58**	**4.18**	***4.08***	**3.00**	**1.83**	**1.55**

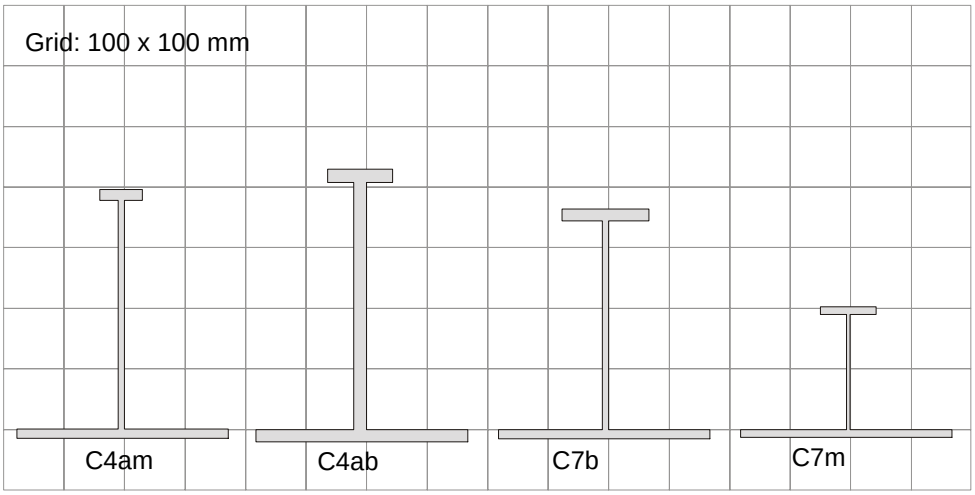

Figure 6. X-sections of the 4 frames in Set 2.

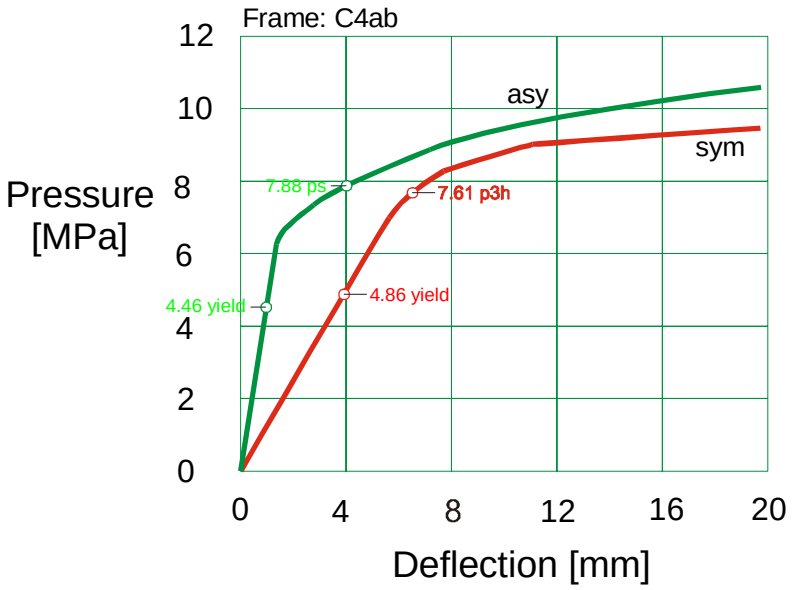

Figure 7 Load-deflection curves for frame C4ab (bow)

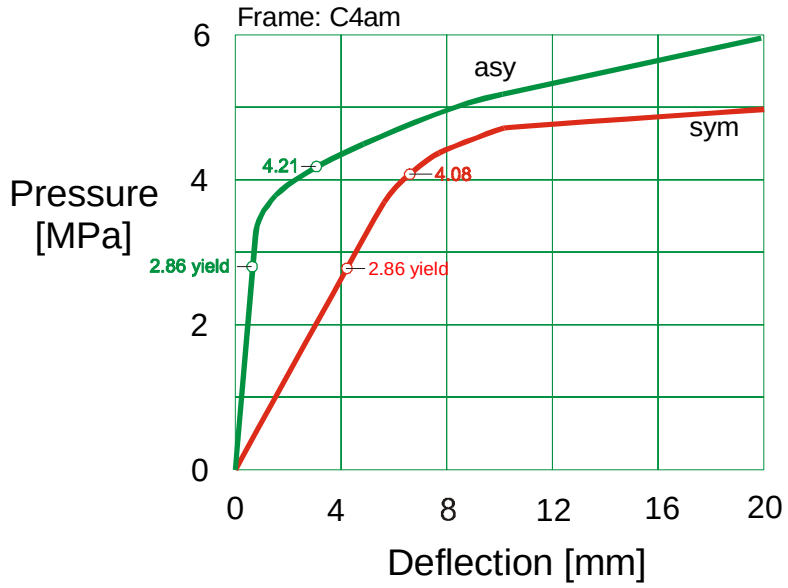

Figure 8 Load-deflection curves for frame C4am (mid)

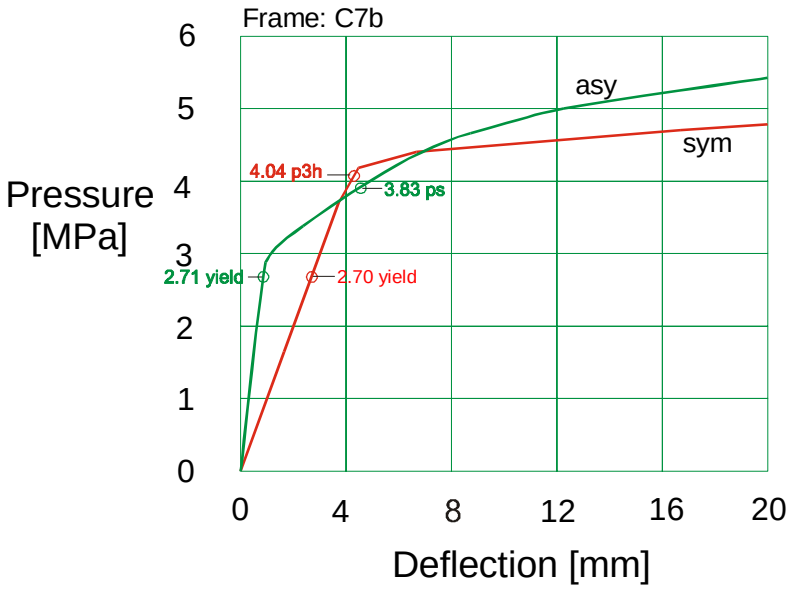

Figure 9. Load-deflection curves for frame C7b (bow)

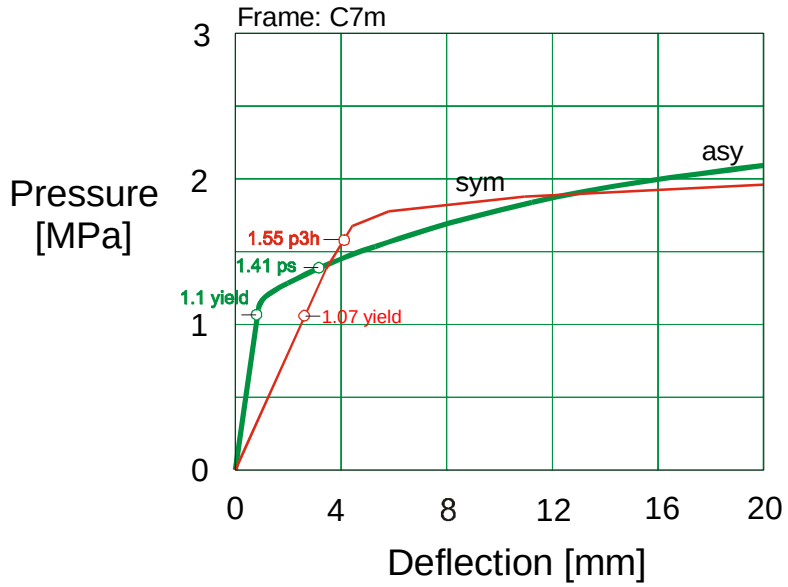

Figure 10. Load-deflection curves for frame C7m (mid)